- **Outstanding Combination of dc Precision and AC Performance:**
  **Unity-Gain Bandwidth . . . 15 MHz Typ**
  **$V_n$ . . . . 3.3 nV/√Hz at f = 10 Hz Typ, 2.5 nV/√Hz at f = 1 kHz Typ**
  **$V_{IO}$ . . . . 25 µV Max**
  **$A_{VD}$ . . . 45 V/µV Typ With $R_L$ = 2 kΩ, 19 V/µV Typ With $R_L$ = 600 Ω**
- **Available in Standard-Pinout Small-Outline Package**
- **Output Features Saturation Recovery Circuitry**
- **Macromodels and Statistical information**

## description

The TLE2027 and TLE2027A contain innovative circuit design expertise and high-quality process control techniques to produce a level of ac performance and dc precision previously unavailable in single operational amplifiers. Manufactured using Texas Instruments state-of-the-art Excalibur process, these devices allow upgrades to systems that use lower-precision devices.

In the area of dc precision, the TLE2027 and TLE2027A offer maximum offset voltages of 100 µV and 25 µV, respectively, common-mode rejection ratio of 131 dB (typ), supply voltage rejection ratio of 144 dB (typ), and dc gain of 45 V/µV (typ).

The ac performance is highlighted by a typical unity-gain bandwidth specification of 15 MHz, 55° of phase margin, and noise voltage specifications of 3.3 nV/√Hz and 2.5 nV/√Hz at frequencies of 10 Hz and 1 kHz respectively.

**LARGE-SIGNAL DIFFERENTIAL VOLTAGE AMPLIFICATION vs FREQUENCY**

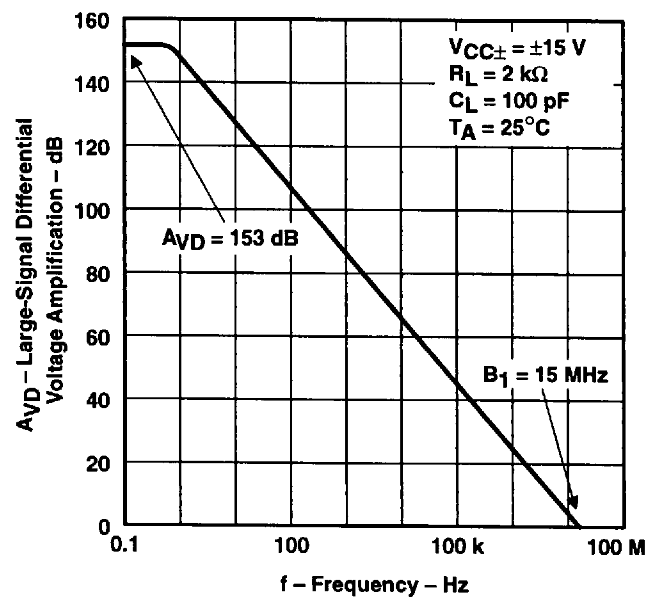


**AVAILABLE OPTIONS**

| $T_A$ | $V_{IO}$max AT 25°C | PACKAGED DEVICES | | | | CHIP FORM (Y) |
|---|---|---|---|---|---|---|
| | | SMALL OUTLINE (D) | CHIP CARRIER (FK) | CERAMIC DIP (JG) | PLASTIC DIP (P) | |
| 0°C to 70°C | 25 µV<br>100 µV | TLE2027ACD<br>TLE2027CD | —<br>— | —<br>— | TLE2027ACP<br>TLE2027CP | —<br>TLE2027Y |
| −40°C to 105°C | 25 µV<br>100 µV | TLE2027AID<br>TLE2027ID | —<br>— | —<br>— | TLE2027AIP<br>TLE2027IP | —<br>— |
| −55°C to 125°C | 25 µV<br>100 µV | TLE2027AMD<br>TLE2027MD | TLE2027AMFK<br>TLE2027MFK | TLE2027AMJG<br>TLE2027MJG | TLE2027AMP<br>TLE2027MP | —<br>— |

The D packages are available taped and reeled. Add R suffix to device type (e.g., TLE2027ACDR).

Please be aware that an important notice concerning availability, standard warranty, and use in critical applications of Texas Instruments semiconductor products and disclaimers thereto appears at the end of this data sheet.

## description (continued)

Both the TLE2027 and TLE2027A are available in a wide variety of packages, including the industry-standard 8-pin small-outline version for high-density system applications. The C-suffix devices are characterized for operation from 0°C to 70°C. The I-suffix devices are characterized for operation from −40°C to 105°C. The M-suffix devices are characterized for operation over the full military temperature range of −55°C to 125°C.

**D, JG, OR P PACKAGE**
**(TOP VIEW)**

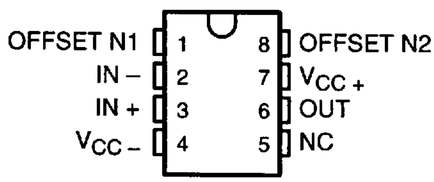


NC – No internal connection

**FK PACKAGE**
**(TOP VIEW)**

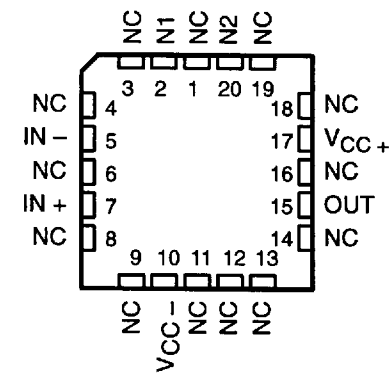


## symbol

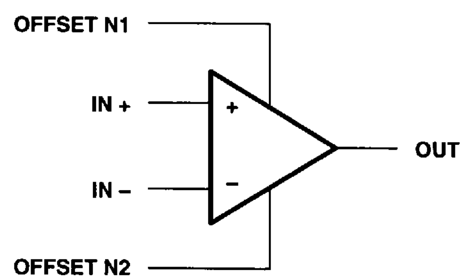

## TLE2027Y chip information

This chip, when properly assembled, displays characteristics similar to the TLE2027C. Thermal compression or ultrasonic bonding may be used on the doped-aluminum bonding pads. The chip may be mounted with conductive epoxy or a gold-silicon preform.

BONDING PAD ASSIGNMENTS

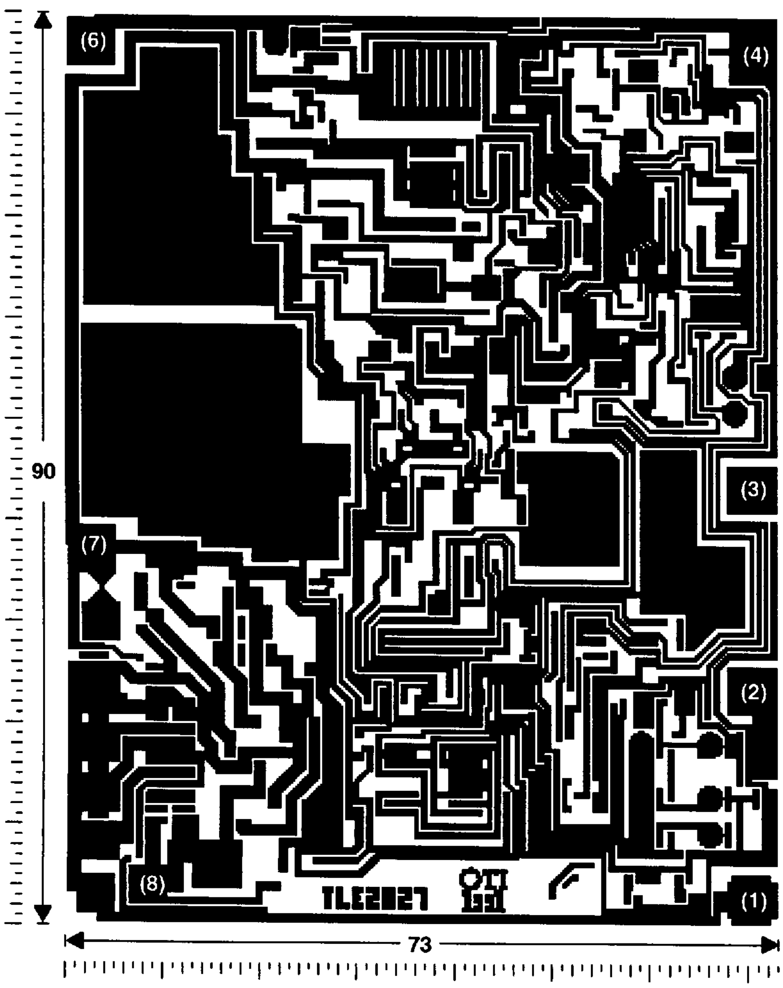


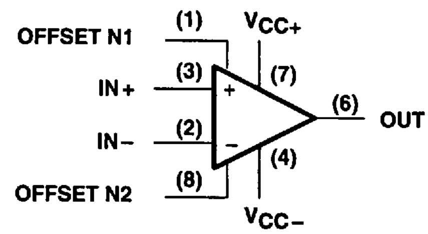


CHIP THICKNESS: 15 MILS TYPICAL

BONDING PADS: 4 × 4 MILS MINIMUM

$T_J$max = 150°C

TOLERANCES ARE ±10%.

ALL DIMENSIONS ARE IN MILS.

PIN (4) IS INTERNALLY CONNECTED TO BACKSIDE OF CHIP.

## equivalent schematic

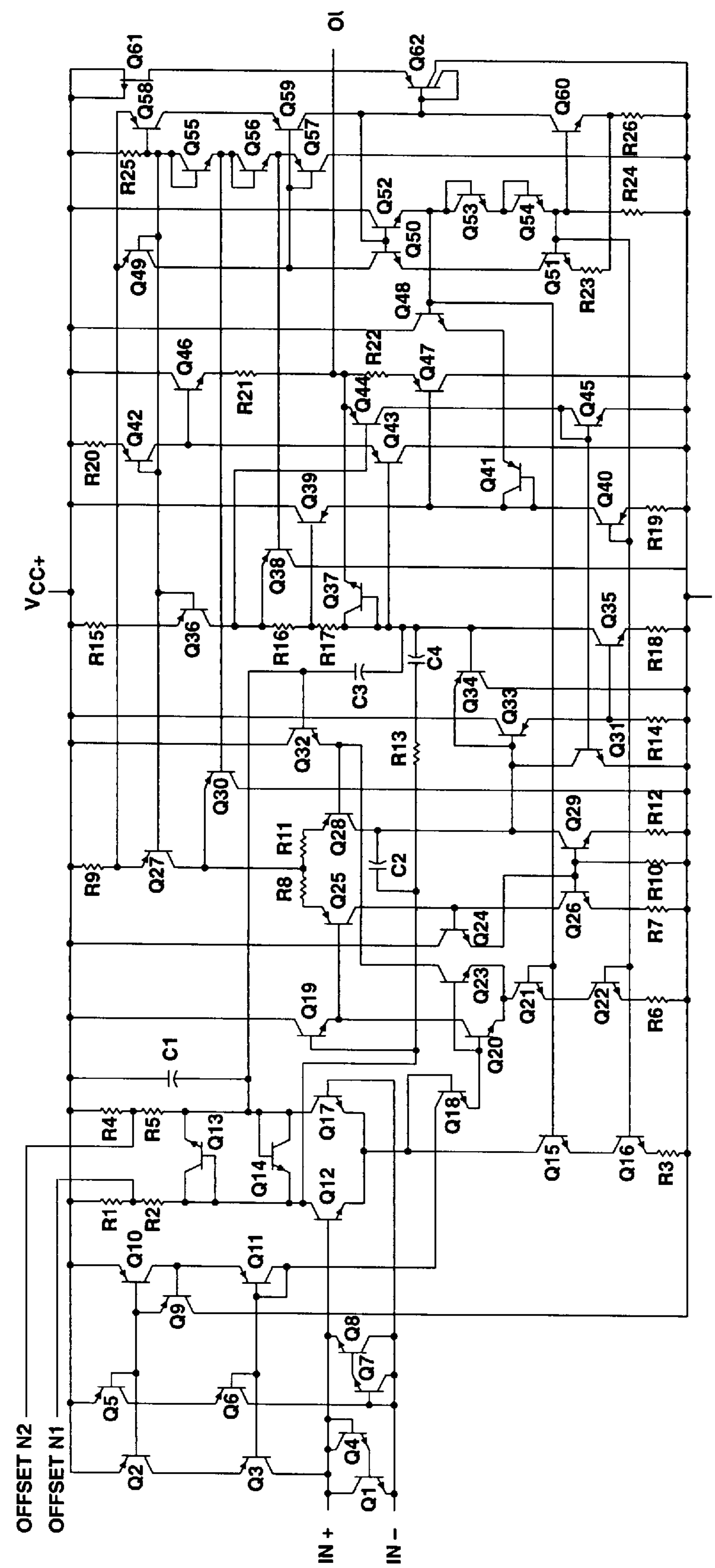


| COMPONENT COUNT | |
|---|---|
| Transistors | 61 |
| Resistors | 26 |
| Capacitors | 4 |
| epi FET | 1 |



TEXAS INSTRUMENTS
POST OFFICE BOX 655303 • DALLAS, TEXAS 75265

8961724 0103600 872

## absolute maximum ratings over operating free-air temperature range (unless otherwise noted)†

| | |
|---|---|
| Supply voltage, $V_{CC+}$ (see Note 1) | 19 V |
| Supply voltage, $V_{CC-}$ | – 19 V |
| Differential input voltage, $V_{ID}$ (see Note 2) | ±1.2 V |
| Input voltage range, $V_I$ (any input) | $V_{CC\pm}$ |
| Input current, $I_I$ (each Input) | ±1 mA |
| Output current, $I_O$ | ± 50 mA |
| Total current into $V_{CC+}$ | 50 mA |
| Total current out of $V_{CC-}$ | 50 mA |
| Duration of short-circuit current at (or below) 25°C (see Note 3) | unlimited |
| Continuous total power dissipation | See Dissipation Rating Table |
| Operating free-air temperature range, $T_A$: C suffix | 0°C to 70°C |
| I suffix | – 40°C to 105°C |
| M suffix | – 55°C to 125°C |
| Storage temperature range, $T_{stg}$ | – 65°C to 150°C |
| Case temperature for 60 seconds, $T_C$: FK package | 260°C |
| Lead temperature 1,6 mm (1/16 inch) from case for 10 seconds: D or P package | 260°C |
| Lead temperature 1,6 mm (1/16 inch) from case for 60 seconds: JG package | 300°C |

† Stresses beyond those listed under "absolute maximum ratings" may cause permanent damage to the device. These are stress ratings only, and functional operation of the device at these or any other conditions beyond those indicated under "recommended operating conditions" is not implied. Exposure to absolute-maximum-rated conditions for extended periods may affect device reliability.

NOTES: 1. All voltage values, except differential voltages, are with respect to the midpoint between $V_{CC+}$ and $V_{CC-}$.
2. Differential voltages are at IN+ with respect to IN–. Excessive current flows if a differential input voltage in excess of approximately ±1.2 V is applied between the inputs unless some limiting resistance is used.
3. The output may be shorted to either supply. Temperature and/or supply voltages must be limited to ensure that the maximum dissipation rating is not exceeded.

**DISSIPATION RATING TABLE**

| PACKAGE | $T_A \le 25°C$ POWER RATING | DERATING FACTOR ABOVE $T_A = 25°C$ | $T_A = 70°C$ POWER RATING | $T_A = 105°C$ POWER RATING | $T_A = 125°C$ POWER RATING |
|---|---|---|---|---|---|
| D | 725 mW | 5.8 mW/°C | 464 mW | 261 mW | 145 mW |
| FK | 1375 mW | 11.0 mW/°C | 880 mW | 495 mW | 275 mW |
| JG | 1050 mW | 8.4 mW/°C | 672 mW | 378 mW | 210 mW |
| P | 1000 mW | 8.0 mW/°C | 640 mW | 360 mW | 200 mW |

## recommended operating conditions

| | | C SUFFIX | | I SUFFIX | | M SUFFIX | | UNIT |
|---|---|---|---|---|---|---|---|---|
| | | MIN | MAX | MIN | MAX | MIN | MAX | |
| Supply voltage, $V_{CC\pm}$ | | ±4 | ± 19 | ±4 | ±19 | ±4 | ±19 | V |
| Common-mode input voltage, $V_{IC}$ | $T_A = 25°C$ | –11 | 11 | –11 | 11 | –11 | 11 | V |
| | $T_A$ = Full range‡ | –10.5 | 10.5 | –10.4 | 10.4 | –10.2 | 10.2 | |
| Operating free-air temperature, $T_A$ | | 0 | 70 | –40 | 105 | –55 | 125 | °C |

‡ Full range is 0°C to 70°C for C-suffix devices, –40°C to 105°C for I-suffix devices, and –55°C to 125°C for M-suffix devices.

## electrical characteristics at specified free-air temperature, $V_{CC\pm}$ = ±15 V (unless otherwise noted)

| PARAMETER | | TEST CONDITIONS | $T_A$† | TLE2027C | | | TLE2027AC | | | UNIT |
|---|---|---|---|---|---|---|---|---|---|---|
| | | | | MIN | TYP | MAX | MIN | TYP | MAX | |
| $V_{IO}$ | Input offset voltage | $V_{IC}$ = 0, $R_S$ = 50 Ω | 25°C | | 20 | 100 | | 10 | 25 | µV |
| | | | Full range | | | 145 | | | 70 | |
| $\alpha_{VIO}$ | Temperature coefficient of input offset voltage | | Full range | | 0.4 | 1 | | 0.2 | 1 | µV/°C |
| | Input offset voltage long-term drift (see Note 4) | | 25°C | | 0.006 | 1 | | 0.006 | 1 | µV/mo |
| $I_{IO}$ | Input offset current | | 25°C | | 6 | 90 | | 6 | 90 | nA |
| | | | Full range | | | 150 | | | 150 | |
| $I_{IB}$ | Input bias current | | 25°C | | 15 | 90 | | 15 | 90 | nA |
| | | | Full range | | | 150 | | | 150 | |
| $V_{ICR}$ | Common-mode input voltage range | $R_S$ = 50 Ω | 25°C | −11 to 11 | −13 to 13 | | −11 to 11 | −13 to 13 | | V |
| | | | Full range | −10.5 to 10.5 | | | −10.5 to 10.5 | | | |
| $V_{OM+}$ | Maximum positive peak output voltage swing | $R_L$ = 600 Ω | 25°C | 10.5 | | | 10.5 | | | V |
| | | | Full range | 10 | | | 10 | | | |
| | | $R_L$ = 2 kΩ | 25°C | 12 | | | 12 | | | |
| | | | Full range | 11 | | | 11 | | | |
| $V_{OM-}$ | Maximum negative peak output voltage swing | $R_L$ = 600 Ω | 25°C | −10.5 | −13 | | −10.5 | −13 | | V |
| | | | Full range | −10 | | | −10 | | | |
| | | $R_L$ = 2 kΩ | 25°C | − 12 | −13.5 | | − 12 | −13.5 | | |
| | | | Full range | − 11 | | | − 11 | | | |
| $A_{VD}$ | Large-signal differential voltage amplification | $V_O$ = ±11 V, $R_L$ = 2 kΩ | 25°C | 5 | 45 | | 10 | 45 | | V/µV |
| | | $V_O$ = ±10 V, $R_L$ = 2 kΩ | Full range | 2 | | | 4 | | | |
| | | $V_O$ = ±10 V, $R_L$ = 1 kΩ | 25°C | 3.5 | 38 | | 8 | 38 | | |
| | | | Full range | 1 | | | 2.5 | | | |
| | | $V_O$ = ±10 V, $R_L$ = 600 Ω | 25°C | 2 | 19 | | 5 | 19 | | |
| | | | Full range | 0.5 | | | 2 | | | |
| $C_i$ | Input capacitance | | 25°C | | 8 | | | 8 | | pF |
| $z_o$ | Open-loop output impedance | $I_O$ = 0 | 25°C | | 50 | | | 50 | | Ω |
| CMRR | Common-mode rejection ratio | $V_{IC}$ = $V_{ICR}$min, $R_S$ = 50 Ω | 25°C | 100 | 131 | | 117 | 131 | | dB |
| | | | Full range | 98 | | | 114 | | | |
| $k_{SVR}$ | Supply-voltage rejection ratio ($\Delta V_{CC\pm}/\Delta V_{IO}$) | $V_{CC\pm}$ = ±4 V to ±18 V, $R_S$ = 50 Ω | 25°C | 94 | 144 | | 110 | 144 | | dB |
| | | $V_{CC\pm}$ = ±4 V to ±18 V, $R_S$ = 50 Ω | Full range | 92 | | | 106 | | | |
| $I_{CC}$ | Supply current | $V_O$ = 0, No load | 25°C | | 3.8 | 5.3 | | 3.8 | 5.3 | mA |
| | | | Full range | | | 5.6 | | | 5.6 | |

† Full range is 0°C to 70°C.

NOTE 4: Typical values are based on the input offset voltage shift observed through 168 hours of operating life test at $T_A$ = 150°C extrapolated to $T_A$ = 25°C using the Arrhenius equation and assuming an activation energy of 0.96 eV.

## operating characteristics at specified free-air temperature, $V_{CC\pm} = \pm 15$ V

| PARAMETER | | TEST CONDITIONS | $T_A$† | TLE2027C | | | TLE2027AC | | | UNIT |
|---|---|---|---|---|---|---|---|---|---|---|
| | | | | MIN | TYP | MAX | MIN | TYP | MAX | |
| SR | Slew rate at unity gain | $R_L = 2\ k\Omega$, $C_L = 100\ pF$, See Figure 1 | 25°C | 1.7 | 2.8 | | 1.7 | 2.8 | | V/μs |
| | | | Full range | 1.2 | | | 1.2 | | | |
| $V_n$ | Equivalent input noise voltage (see Figure 2) | $R_S = 20\ \Omega$, f = 10 Hz | 25°C | | 3.3 | 8 | | 3.3 | 4.5 | nV/√Hz |
| | | $R_S = 20\ \Omega$, f = 1 kHz | | | 2.5 | 4.5 | | 2.5 | 3.8 | |
| $V_{N(PP)}$ | Peak-to-peak equivalent input noise voltage | f = 0.1 Hz to 10 Hz | 25°C | | 50 | 250 | | 50 | 130 | nV |
| $I_n$ | Equivalent input noise current | f = 10 Hz | 25°C | | 1.5 | 4 | | 1.5 | 4 | pA/√Hz |
| | | f = 1 kHz | | | 0.4 | 0.6 | | 0.4 | 0.6 | |
| THD | Total harmonic distortion | $V_O = +10$ V, $A_{VD} = 5$, See Note 5 | 25°C | | <0.002% | | | <0.002% | | |
| $B_1$ | Unity-gain bandwidth (see Figure 3) | $R_L = 2\ k\Omega$, $C_L = 100\ pF$ | 25°C | 7 | 13 | | 9 | 13 | | MHz |
| $B_{OM}$ | Maximum output-swing bandwidth | $R_L = 2\ k\Omega$ | 25°C | | 30 | | | 30 | | kHz |
| $\phi_m$ | Phase margin at unity gain (see Figure 3) | $R_L = 2\ k\Omega$, $C_L = 100\ pF$ | 25°C | | 55° | | | 55° | | |

† Full range is 0°C to 70°C.
NOTE 5: Measured distortion of the source used in the analysis was 0.002%.

## electrical characteristics at specified free-air temperature, $V_{CC\pm} = \pm 15$ V (unless otherwise noted)

| PARAMETER | | TEST CONDITIONS | $T_A$† | TLE2027I | | | TLE2027AI | | | UNIT |
|---|---|---|---|---|---|---|---|---|---|---|
| | | | | MIN | TYP | MAX | MIN | TYP | MAX | |
| $V_{IO}$ | Input offset voltage | $V_{IC} = 0$, $R_S = 50\ \Omega$ | 25°C | | 20 | 100 | | 10 | 25 | µV |
| | | | Full range | | | 180 | | | 105 | |
| $\alpha_{VIO}$ | Temperature coefficient of input offset voltage | | Full range | | 0.4 | 1 | | 0.2 | 1 | µV/°C |
| | Input offset voltage long-term drift (see Note 4) | | 25°C | | 0.006 | 1 | | 0.006 | 1 | µV/mo |
| $I_{IO}$ | Input offset current | | 25°C | | 6 | 90 | | 6 | 90 | nA |
| | | | Full range | | | 150 | | | 150 | |
| $I_{IB}$ | Input bias current | | 25°C | | 15 | 90 | | 15 | 90 | nA |
| | | | Full range | | | 150 | | | 150 | |
| $V_{ICR}$ | Common-mode input voltage range | $R_S = 50\ \Omega$ | 25°C | −11 to 11 | −13 to 13 | | −11 to 11 | −13 to 13 | | V |
| | | | Full range | −10.4 to 10.4 | | | −10.4 to 10.4 | | | |
| $V_{OM+}$ | Maximum positive peak output voltage swing | $R_L = 600\ \Omega$ | 25°C | 10.5 | | | 10.5 | | | V |
| | | | Full range | 10 | | | 10 | | | |
| | | $R_L = 2\ k\Omega$ | 25°C | 12 | | | 12 | | | |
| | | | Full range | 11 | | | 11 | | | |
| $V_{OM-}$ | Maximum negative peak output voltage swing | $R_L = 600\ \Omega$ | 25°C | −10.5 | −13 | | −10.5 | −13 | | V |
| | | | Full range | −10 | | | −10 | | | |
| | | $R_L = 2\ k\Omega$ | 25°C | − 12 | −13.5 | | − 12 | −13.5 | | |
| | | | Full range | − 11 | | | − 11 | | | |
| $A_{VD}$ | Large-signal differential voltage amplification | $V_O = \pm 11$ V, $R_L = 2\ k\Omega$ | 25°C | 5 | 45 | | 10 | 45 | | V/µV |
| | | $V_O = \pm 10$ V, $R_L = 2\ k\Omega$ | Full range | 2 | | | 3.5 | | | |
| | | $V_O = \pm 10$ V, $R_L = 1\ k\Omega$ | 25°C | 3.5 | 38 | | 8 | 38 | | |
| | | | Full range | 1 | | | 2.2 | | | |
| | | $V_O = \pm 10$ V, $R_L = 600\ \Omega$ | 25°C | 2 | 19 | | 5 | 19 | | |
| | | | Full range | 0.5 | | | 1.1 | | | |
| $C_i$ | Input capacitance | | 25°C | | 8 | | | 8 | | pF |
| $z_o$ | Open-loop output impedance | $I_O = 0$ | 25°C | | 50 | | | 50 | | Ω |
| CMRR | Common-mode rejection ratio | $V_{IC} = V_{ICR}$min, $R_S = 50\ \Omega$ | 25°C | 100 | 131 | | 117 | 131 | | dB |
| | | | Full range | 96 | | | 113 | | | |
| $k_{SVR}$ | Supply-voltage rejection ratio ($\Delta V_{CC\pm} / \Delta V_{IO}$) | $V_{CC\pm} = \pm 4$ V to $\pm 18$ V, $R_S = 50\ \Omega$ | 25°C | 94 | 144 | | 110 | 144 | | dB |
| | | $V_{CC\pm} = \pm 4$ V to $\pm 18$ V, $R_S = 50\ \Omega$ | Full range | 90 | | | 105 | | | |
| $I_{CC}$ | Supply current | $V_O = 0$, No load | 25°C | | 3.8 | 5.3 | | 3.8 | 5.3 | mA |
| | | | Full range | | | 5.6 | | | 5.6 | |

† Full range is – 40°C to 105°C.

NOTE 4: Typical values are based on the input offset voltage shift observed through 168 hours of operating life test at $T_A = 150°C$ extrapolated to $T_A = 25°C$ using the Arrhenius equation and assuming an activation energy of 0.96 eV.

## operating characteristics at specified free-air temperature, $V_{CC\pm} = \pm15$ V

| PARAMETER | | TEST CONDITIONS | $T_A$† | TLE2027I | | | TLE2027AI | | | UNIT |
|---|---|---|---|---|---|---|---|---|---|---|
| | | | | MIN | TYP | MAX | MIN | TYP | MAX | |
| SR | Slew rate at unity gain | $R_L = 2$ kΩ, $C_L = 100$ pF, See Figure 1 | 25°C | 1.7 | 2.8 | | 1.7 | 2.8 | | V/μs |
| | | | Full range | 1.1 | | | 1.1 | | | |
| $V_n$ | Equivalent input noise voltage (see Figure 2) | $R_S = 20$ Ω, f = 10 Hz | 25°C | | 3.3 | 8 | | 3.3 | 4.5 | nV/√Hz |
| | | $R_S = 20$ Ω, f = 1 kHz | | | 2.5 | 4.5 | | 2.5 | 3.8 | |
| $V_{N(PP)}$ | Peak-to-peak equivalent input noise voltage | f = 0.1 Hz to 10 Hz | 25°C | | 50 | 250 | | 50 | 130 | nV |
| $I_n$ | Equivalent input noise current | f = 10 Hz | 25°C | | 1.5 | 4 | | 1.5 | 4 | pA/√Hz |
| | | f = 1 kHz | | | 0.4 | 0.6 | | 0.4 | 0.6 | |
| THD | Total harmonic distortion | $V_O = +10$ V, $A_{VD} = 1$, See Note 5 | 25°C | | < 0.002% | | | < 0.002% | | |
| $B_1$ | Unity-gain bandwidth (see Figure 3) | $R_L = 2$ kΩ, $C_L = 100$ pF | 25°C | 7 | 13 | | 9 | 13 | | MHz |
| $B_{OM}$ | Maximum output-swing bandwidth | $R_L = 2$ kΩ | 25°C | | 30 | | | 30 | | kHz |
| $\phi_m$ | Phase margin at unity gain (see Figure 3) | $R_L = 2$ kΩ, $C_L = 100$ pF | 25°C | | 55° | | | 55° | | |

† Full range is – 40°C to 105°C.
NOTE 5: Measured distortion of the source used in the analysis was 0.002%.

## electrical characteristics at specified free-air temperature, $V_{CC\pm} = \pm15$ V (unless otherwise noted)

| PARAMETER | | TEST CONDITIONS | $T_A$† | TLE2027M | | | TLE2027AM | | | UNIT |
|---|---|---|---|---|---|---|---|---|---|---|
| | | | | MIN | TYP | MAX | MIN | TYP | MAX | |
| $V_{IO}$ | Input offset voltage | $V_{IC} = 0$, $R_S = 50\ \Omega$ | 25°C | | 20 | 100 | | 10 | 25 | μV |
| | | | Full range | | | 200 | | | 105 | |
| $\alpha_{VIO}$ | Temperature coefficient of input offset voltage | | Full range | | 0.4 | 1* | | 0.2 | 1* | μV/°C |
| | Input offset voltage long-term drift (see Note 4) | | 25°C | | 0.006 | 1* | | 0.006 | 1* | μV/mo |
| $I_{IO}$ | Input offset current | | 25°C | | 6 | 90 | | 6 | 90 | nA |
| | | | Full range | | | 150 | | | 150 | |
| $I_{IB}$ | Input bias current | | 25°C | | 15 | 90 | | 15 | 90 | nA |
| | | | Full range | | | 150 | | | 150 | |
| $V_{ICR}$ | Common-mode input voltage range | $R_S = 50\ \Omega$ | 25°C | −11 to 11 | −13 to 13 | | −11 to 11 | −13 to 13 | | V |
| | | | Full range | −10.3 to 10.3 | | | −10.4 to 10.4 | | | |
| $V_{OM+}$ | Maximum positive peak output voltage swing | $R_L = 600\ \Omega$ | 25°C | 10.5 | | | 10.5 | | | V |
| | | | Full range | 10 | | | 10 | | | |
| | | $R_L = 2\ k\Omega$ | 25°C | 12 | | | 12 | | | |
| | | | Full range | 11 | | | 11 | | | |
| $V_{OM-}$ | Maximum negative peak output voltage swing | $R_L = 600\ \Omega$ | 25°C | −10.5 | −13 | | −10.5 | −13 | | V |
| | | | Full range | −10 | | | −10 | | | |
| | | $R_L = 2\ k\Omega$ | 25°C | −12 | −13.5 | | −12 | −13.5 | | |
| | | | Full range | −11 | | | −11 | | | |
| $A_{VD}$ | Large-signal differential voltage amplification | $V_O = \pm11$ V, $R_L = 2\ k\Omega$ | 25°C | 5 | 45 | | 10 | 45 | | V/μV |
| | | $V_O = \pm10$ V, $R_L = 2\ k\Omega$ | Full range | 2.5 | | | 3.5 | | | |
| | | $V_O = \pm10$ V, $R_L = 1\ k\Omega$ | 25°C | 3.5 | 38 | | 8 | 38 | | |
| | | | Full range | 1.8 | | | 2.2 | | | |
| | | $V_O = \pm10$ V, $R_L = 600\ \Omega$ | 25°C | 2 | 19 | | 5 | 19 | | |
| $C_i$ | Input capacitance | | 25°C | | 8 | | | 8 | | pF |
| $z_o$ | Open-loop output impedance | $I_O = 0$ | 25°C | | 50 | | | 50 | | Ω |
| CMRR | Common-mode rejection ratio | $V_{IC} = V_{ICR}$min, $R_S = 50\ \Omega$ | 25°C | 100 | 131 | | 117 | 131 | | dB |
| | | | Full range | 96 | | | 113 | | | |
| $k_{SVR}$ | Supply-voltage rejection ratio ($\Delta V_{CC\pm}/\Delta V_{IO}$) | $V_{CC\pm} = \pm4$ V to $\pm18$ V, $R_S = 50\ \Omega$ | 25°C | 94 | 144 | | 110 | 144 | | dB |
| | | $V_{CC\pm} = \pm4$ V to $\pm18$ V, $R_S = 50\ \Omega$ | Full range | 90 | | | 105 | | | |
| $I_{CC}$ | Supply current | $V_O = 0$, No load | 25°C | | 3.8 | 5.3 | | 3.8 | 5.3 | mA |
| | | | Full range | | | 5.6 | | | 5.6 | |

* On products compliant to MIL-PRF-38535, this parameter is not production tested.
† Full range is – 55°C to 125°C.
NOTE 4: Typical values are based on the input offset voltage shift observed through 168 hours of operating life test at $T_A = 150°C$ extrapolated to $T_A = 25°C$ using the Arrhenius equation and assuming an activation energy of 0.96 eV.

## operating characteristics at specified free-air temperature, $V_{CC\pm} = \pm 15$ V

| PARAMETER | | TEST CONDITIONS | $T_A$† | TLE2027M | | | TLE2027AM | | | UNIT |
|---|---|---|---|---|---|---|---|---|---|---|
| | | | | MIN | TYP | MAX | MIN | TYP | MAX | |
| SR | Slew rate at unity gain | $R_L = 2$ kΩ, $C_L = 100$ pF, See Figure 1 | 25°C | 1.7 | 2.8 | | 1.7 | 2.8 | | V/μs |
| | | | Full range | 1 | | | 1 | | | |
| $V_n$ | Equivalent input noise voltage (see Figure 2) | $R_S = 20\ \Omega$, f = 10 Hz | 25°C | | 3.3 | 8* | | 3.3 | 4.5* | nV/√Hz |
| | | $R_S = 20\ \Omega$, f = 1 kHz | | | 2.5 | 4.5* | | 2.5 | 3.8* | |
| $V_{N(PP)}$ | Peak-to-peak equivalent input noise voltage | f = 0.1 Hz to 10 Hz | 25°C | | 50 | 250* | | 50 | 130* | nV |
| $I_n$ | Equivalent input noise current | f = 10 Hz | 25°C | | 1.5 | 4* | | 1.5 | 4* | pA/√Hz |
| | | f = 1 kHz | | | 0.4 | 0.6* | | 0.4 | 0.6* | |
| THD | Total harmonic distortion | $V_O = +10$ V, $A_{VD} = 1$, See Note 5 | 25°C | | < 0.002% | | | < 0.002% | | |
| $B_1$ | Unity-gain bandwidth (see Figure 3) | $R_L = 2$ kΩ, $C_L = 100$ pF | 25°C | 7* | 13 | | 9* | 13 | | MHz |
| $B_{OM}$ | Maximum output-swing bandwidth | $R_L = 2$ kΩ | 25°C | | 30 | | | 30 | | kHz |
| $\phi_m$ | Phase margin at unity gain (see Figure 3) | $R_L = 2$ kΩ, $C_L = 100$ pF | 25°C | | 55° | | | 55° | | |

* On products compliant to MIL-PRF-38535, this parameter is not production tested.
† Full range is – 55°C to 125°C.
NOTE 5: Measured distortion of the source used in the analysis was 0.002%.

## electrical characteristics, $V_{CC\pm} = \pm15$ V, $T_A = 25°C$ (unless otherwise noted)

| PARAMETER | | TEST CONDITIONS | TLE2027Y MIN | TLE2027Y TYP | TLE2027Y MAX | UNIT |
|---|---|---|---|---|---|---|
| $V_{IO}$ | Input offset voltage | $V_{IC} = 0$, $R_S = 50\ \Omega$ | | 20 | 100 | µV |
| | Input offset voltage long-term drift (see Note 4) | $V_{IC} = 0$, $R_S = 50\ \Omega$ | | 0.006 | | µV/mo |
| $I_{IO}$ | Input offset current | $V_{IC} = 0$, $R_S = 50\ \Omega$ | | 6 | | nA |
| $I_{IB}$ | Input bias current | $V_{IC} = 0$, $R_S = 50\ \Omega$ | | 15 | | nA |
| $V_{ICR}$ | Common-mode input voltage range | $R_S = 50\ \Omega$ | | −13 to 13 | | V |
| $V_{OM-}$ | Maximum negative peak output voltage swing | $R_L = 600\ \Omega$ | | −13 | | V |
| | | $R_L = 2\ k\Omega$ | | −13.5 | | |
| $A_{VD}$ | Large-signal differential voltage amplification | $V_O = \pm11$ V, $R_L = 2\ k\Omega$ | | 45 | | V/µV |
| | | $V_O = \pm10$ V, $R_L = 1\ k\Omega$ | | 38 | | |
| | | $V_O = \pm10$ V, $R_L = 600\ \Omega$ | | 19 | | |
| $C_i$ | Input capacitance | | | 8 | | pF |
| $z_o$ | Open-loop output impedance | $I_O = 0$ | | 50 | | Ω |
| CMRR | Common-mode rejection ratio | $V_{IC} = V_{ICR}$min, $R_S = 50\ \Omega$ | | 131 | | dB |
| $k_{SVR}$ | Supply-voltage rejection ratio ($\Delta V_{CC\pm}/\Delta V_{IO}$) | $V_{CC\pm} = \pm4$ V to $\pm18$ V, $R_S = 50\ \Omega$ | | 144 | | dB |
| $I_{CC}$ | Supply current | $V_O = 0$, No load | | 3.8 | | mA |

NOTE 4: Typical values are based on the input offset voltage shift observed through 168 hours of operating life test at $T_A = 150°C$ extrapolated to $T_A = 25°C$ using the Arrhenius equation and assuming an activation energy of 0.96 eV.

## operating characteristics at specified free-air temperature, $V_{CC\pm} = \pm15$ V

| PARAMETER | | TEST CONDITIONS | TLE2027Y | | | UNIT |
|---|---|---|---|---|---|---|
| | | | MIN | TYP | MAX | |
| SR | Slew rate at unity gain | $R_L = 2\ k\Omega$, $C_L = 100$ pF, See Figure 1 | | 2.8 | | V/μs |
| $V_n$ | Equivalent input noise voltage (see Figure 2) | $R_S = 20\ \Omega$, f = 10 Hz | | 3.3 | | $nV/\sqrt{Hz}$ |
| | | $R_S = 20\ \Omega$, f = 1 kHz | | 2.5 | | |
| $V_{N(PP)}$ | Peak-to-peak equivalent input noise voltage | f = 0.1 Hz to 10 Hz | | 50 | | nV |
| $I_n$ | Equivalent input noise current | f = 10 Hz | | 1.5 | | $pA/\sqrt{Hz}$ |
| | | f = 1 kHz | | 0.4 | | |
| THD | Total harmonic distortion | $V_O = +10$ V, $A_{VD} = 5$, See Note 5 | | <0.002% | | |
| $B_1$ | Unity-gain bandwidth (see Figure 3) | $R_L = 2\ k\Omega$, $C_L = 100$ pF | | 13 | | MHz |
| $B_{OM}$ | Maximum output-swing bandwidth | $R_L = 2\ k\Omega$ | | 30 | | kHz |
| $\phi_m$ | Phase margin at unity gain (see Figure 3) | $R_L = 2\ k\Omega$, $C_L = 100$ pF | | 55° | | |

NOTE 5: Measured distortion of the source used in the analysis was 0.002%.

## PARAMETER MEASUREMENT INFORMATION

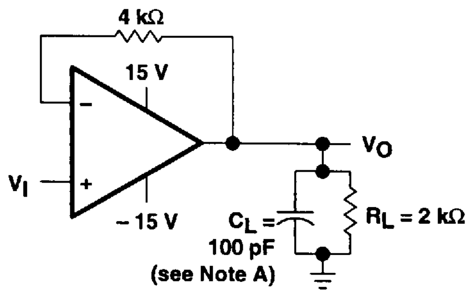


NOTE A: $C_L$ includes fixture capacitance.

**Figure 1. Slew-Rate Test Circuit**

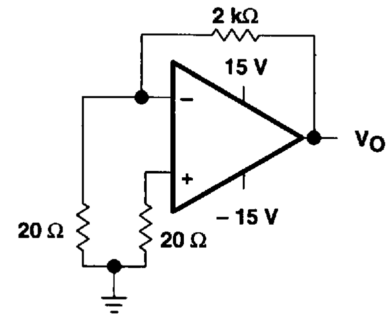


**Figure 2. Noise-Voltage Test Circuit**

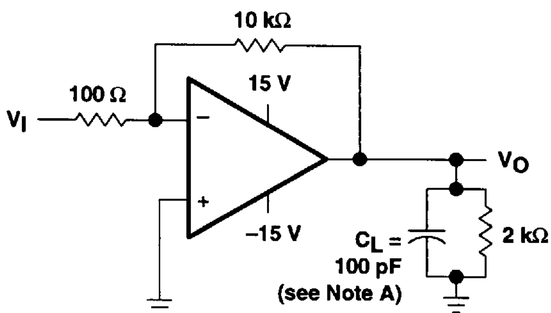


NOTE A: $C_L$ includes fixture capacitance.

**Figure 3. Unity-Gain Bandwidth and Phase-Margin Test Circuit**

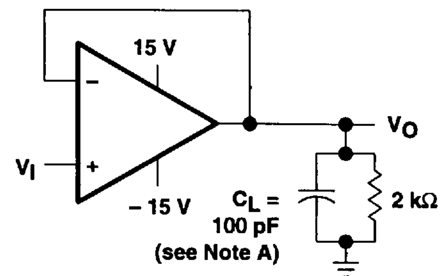


NOTE A: $C_L$ includes fixture capacitance.

**Figure 4. Small-Signal Pulse-Response Test Circuit**

## typical values

Typical values presented in this data sheet represent the median (50% point) of device parametric performance.

## initial estimates of parameter distributions

In the ongoing program of improving data sheets and supplying more information to our customers, Texas Instruments has added an estimate of not only the typical values but also the spread around these values. These are in the form of distribution bars that show the 95% (upper) points and the 5% (lower) points from the characterization of the initial wafer lots of this new device type (see Figure 5). The distribution bars are shown at the points where data was actually collected. The 95% and 5% points are used instead of ± 3 sigma since some of the distributions are not true Gaussian distributions.

The number of units tested and the number of different wafer lots used are on all of the graphs where distribution bars are shown. As noted in Figure 5, there were a total of 835 units from two wafer lots. In this case, there is a good estimate for the within-lot variability and a possibly poor estimate of the lot-to-lot variability. This is always the case on newly released products since there can only be data available from a few wafer lots.

The distribution bars are not intended to replace the minimum and maximum limits in the electrical tables. Each distribution bar represents 90% of the total units tested at a specific temperature. While 10% of the units tested fell outside any given distribution bar, this should not be interpreted to mean that the same individual devices fell outside every distribution bar.

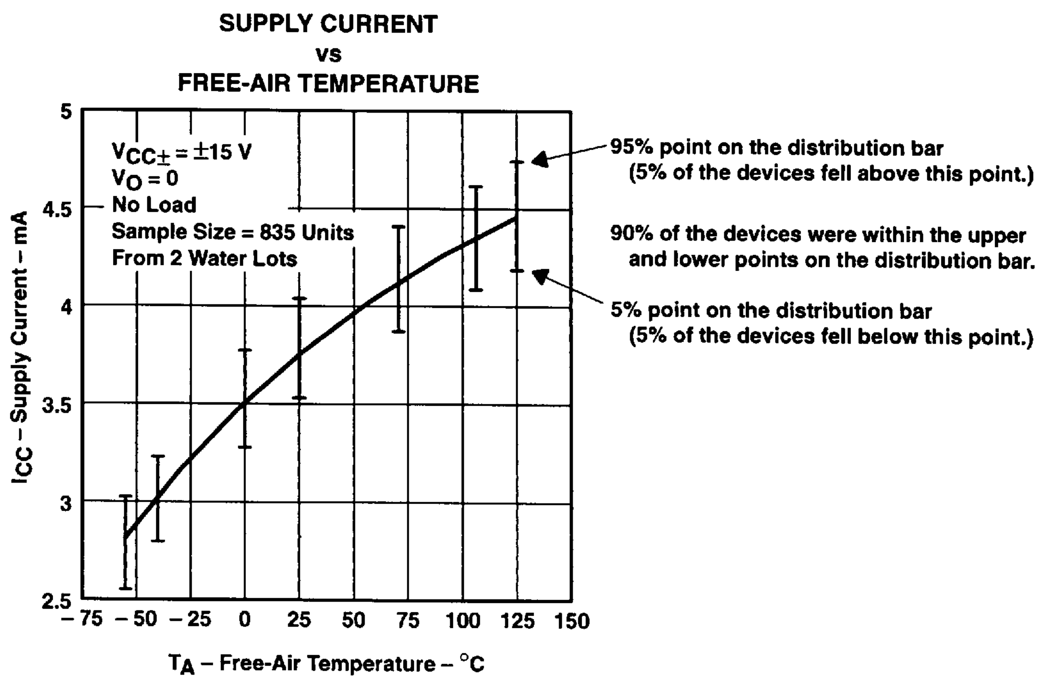


**Figure 5. Sample Graph With Distribution Bars**

## TYPICAL CHARACTERISTICS

### Table of Graphs

| | | | FIGURE |
|---|---|---|---|
| $V_{IO}$ | Input offset voltage | Distribution | 6 |
| $\Delta V_{IO}$ | Input offset voltage change | vs Time after power on | 7, 8 |
| $I_{IO}$ | Input offset current | vs Free-air temperature | 9 |
| $I_{IB}$ | Input bias current | vs Common-mode input voltage<br>vs Free-air temperature | 10<br>11 |
| $I_I$ | Input current | vs Differential input voltage | 12 |
| $V_{O(PP)}$ | Maximum peak-to-peak output voltage | vs Frequency | 13 |
| $V_{OM}$ | Maximum (positive/negative) peak output voltage | vs Load resistance<br>vs Free-air temperature | 14, 15<br>16, 17 |
| $A_{VD}$ | Large-signal differential voltage amplification | vs Supply voltage<br>vs Load resistance<br>vs Frequency<br>vs Free-air temperature | 18<br>19<br>20, 21<br>22 |
| $z_o$ | Output impedance | vs Frequency | 23 |
| CMRR | Common-mode rejection ratio | vs Frequency | 24 |
| $k_{SVR}$ | Supply voltage rejection ratio | vs Frequency | 25 |
| $I_{OS}$ | Short-circuit output current | vs Supply voltage<br>vs Elapsed time<br>vs Free-air temperature | 26, 27<br>28, 29<br>30, 31 |
| $I_{CC}$ | Supply current | vs Supply voltage<br>vs Free-air temperature | 32<br>33 |
| | Pulse response | Small signal<br>Large signal | 34<br>35 |
| $V_n$ | Equivalent input noise voltage | vs Frequency | 36 |
| | Noise voltage (referred to input) | vs Time | 37 |
| $B_1$ | Unity-gain bandwidth | vs Supply voltage<br>vs Load capacitance | 38<br>39 |
| SR | Slew rate | vs Free-air temperature | 40 |
| $\phi_m$ | Phase margin | vs Supply voltage<br>vs Load capacitance<br>vs Free-air temperature | 41<br>42<br>43 |
| | Phase shift | vs Frequency | 20, 21 |

## TYPICAL CHARACTERISTICS

TLE2027
DISTRIBUTION
INPUT OFFSET VOLTAGE

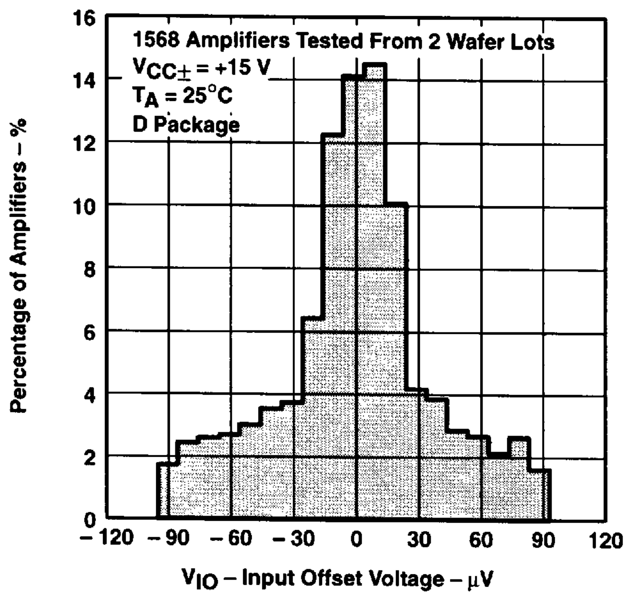


Figure 6

INPUT OFFSET VOLTAGE CHANGE
vs
TIME AFTER POWER ON

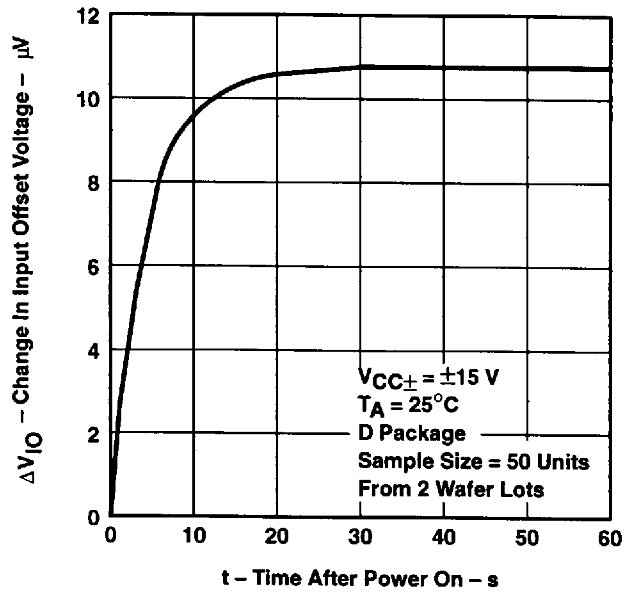


Figure 7

INPUT OFFSET VOLTAGE CHANGE
vs
TIME AFTER POWER ON

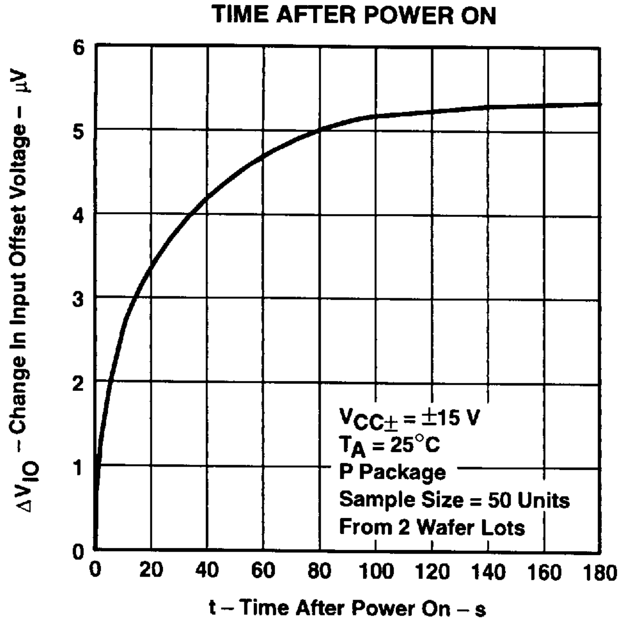


Figure 8

INPUT OFFSET CURRENT†
vs
FREE-AIR TEMPERATURE

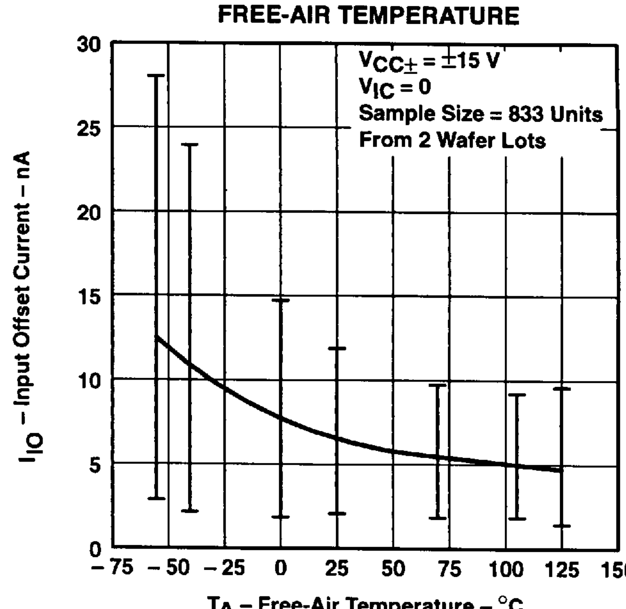


† Data at high and low temperatures are applicable only within the rated operating free-air temperature ranges of the various devices.

Figure 9

## TYPICAL CHARACTERISTICS

**INPUT BIAS CURRENT vs COMMON-MODE INPUT VOLTAGE**

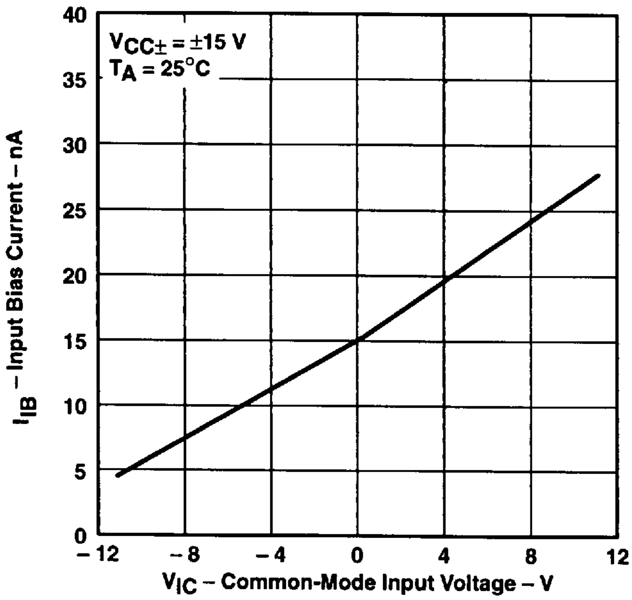


**Figure 10**

**INPUT BIAS CURRENT† vs FREE-AIR TEMPERATURE**

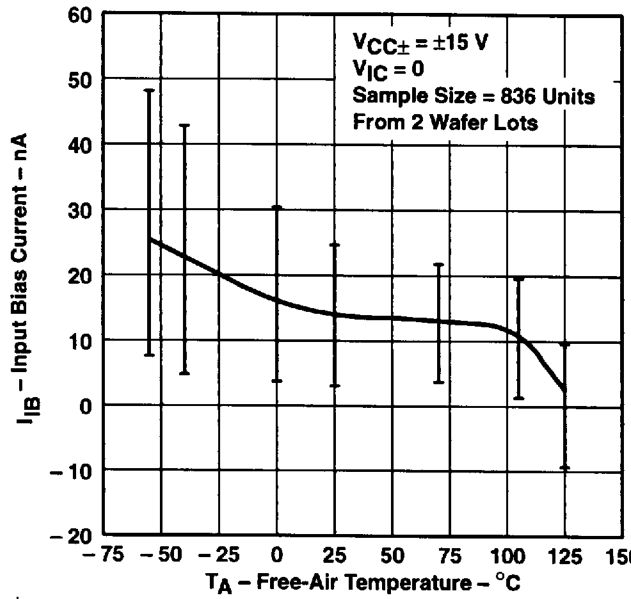


† Data at high and low temperatures are applicable only within the rated operating free-air temperature ranges of the various devices.

**Figure 11**

## TYPICAL CHARACTERISTICS

### INPUT CURRENT vs DIFFERENTIAL INPUT VOLTAGE

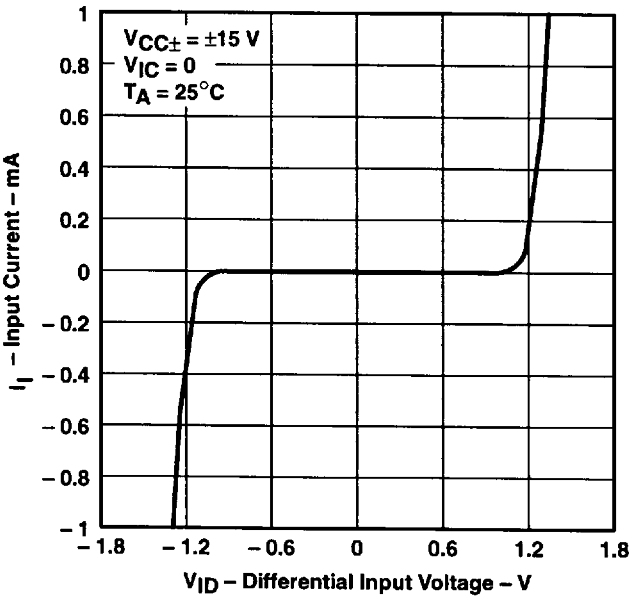


Figure 12

### MAXIMUM PEAK-TO-PEAK OUTPUT VOLTAGE† vs FREQUENCY

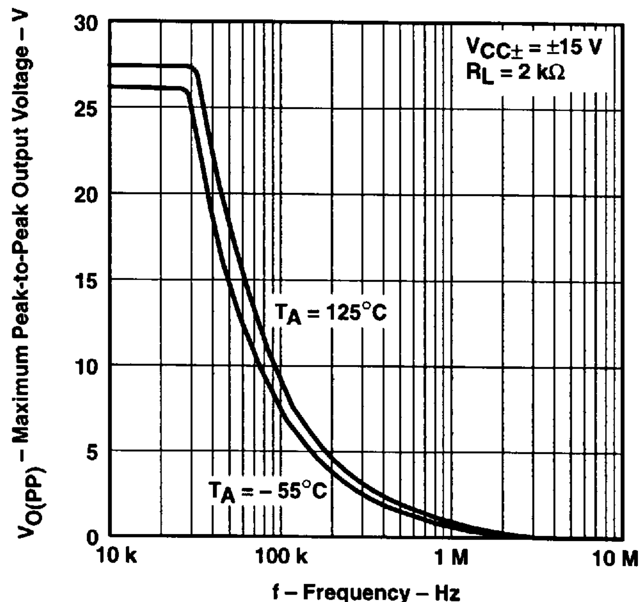


† Data at high and low temperatures are applicable only within the rated operating free-air temperature ranges of the various devices.

Figure 13

## TYPICAL CHARACTERISTICS

**MAXIMUM POSITIVE PEAK OUTPUT VOLTAGE vs LOAD RESISTANCE**

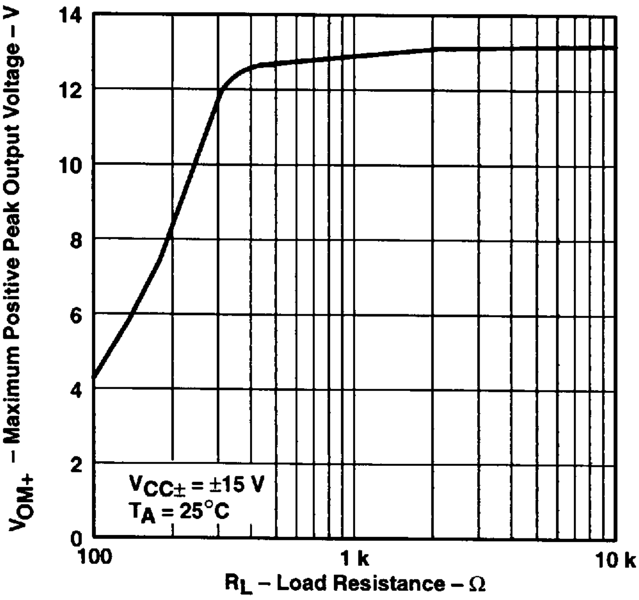


**Figure 14**

**MAXIMUM NEGATIVE PEAK OUTPUT VOLTAGE vs LOAD RESISTANCE**

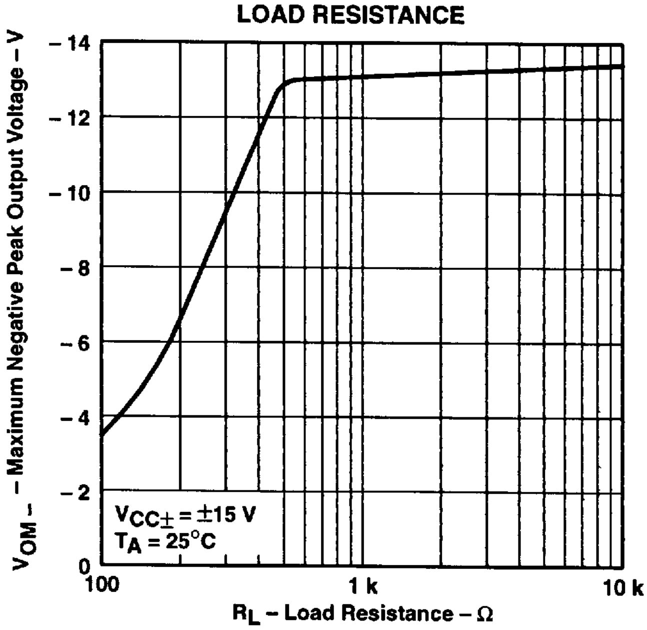


**Figure 15**



TEXAS INSTRUMENTS
POST OFFICE BOX 655303 • DALLAS, TEXAS 75265

## TYPICAL CHARACTERISTICS

**MAXIMUM POSITIVE PEAK OUTPUT VOLTAGE† vs FREE-AIR TEMPERATURE**

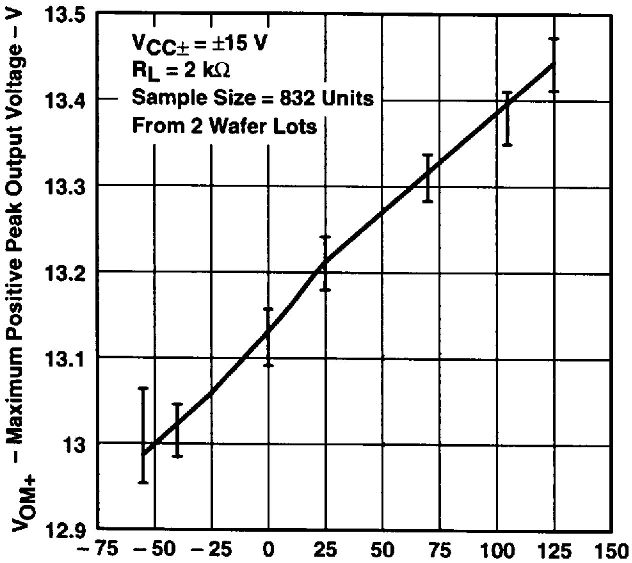


† Data at high and low temperatures are applicable only within the rated operating free-air temperature ranges of the various devices.

**Figure 16**

**MAXIMUM NEGATIVE PEAK OUTPUT VOLTAGE† vs FREE-AIR TEMPERATURE**

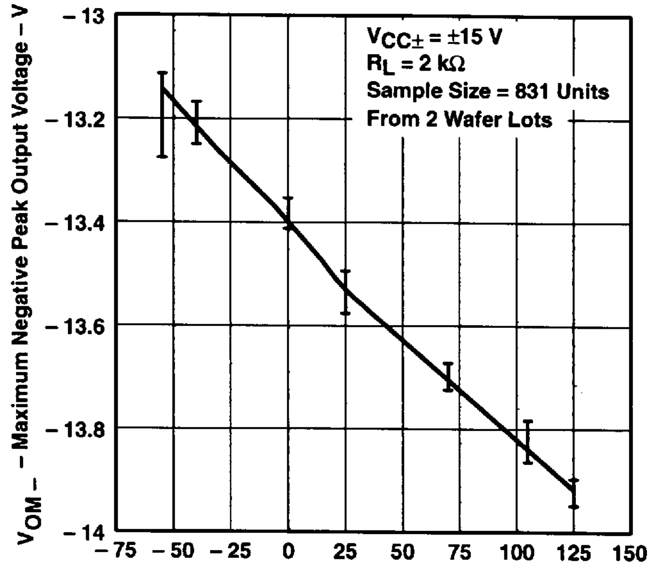


† Data at high and low temperatures are applicable only within the rated operating free-air temperature ranges of the various devices.

**Figure 17**

## TYPICAL CHARACTERISTICS

LARGE-SIGNAL DIFFERENTIAL VOLTAGE AMPLIFICATION vs SUPPLY VOLTAGE

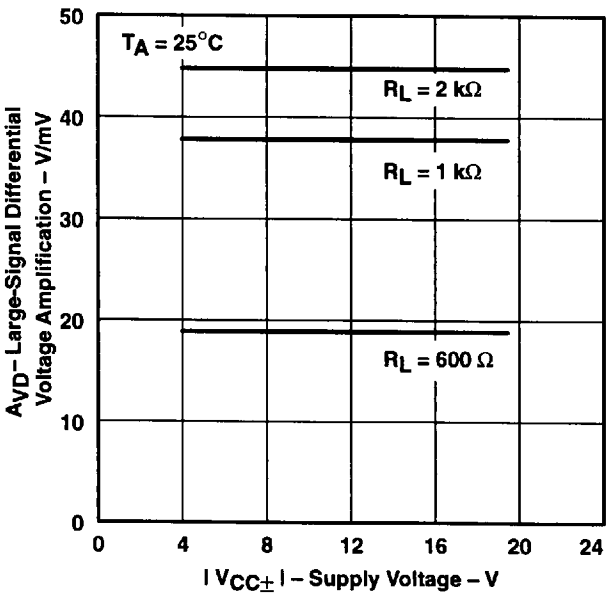


Figure 18

LARGE-SIGNAL DIFFERENTIAL VOLTAGE AMPLIFICATION vs LOAD RESISTANCE

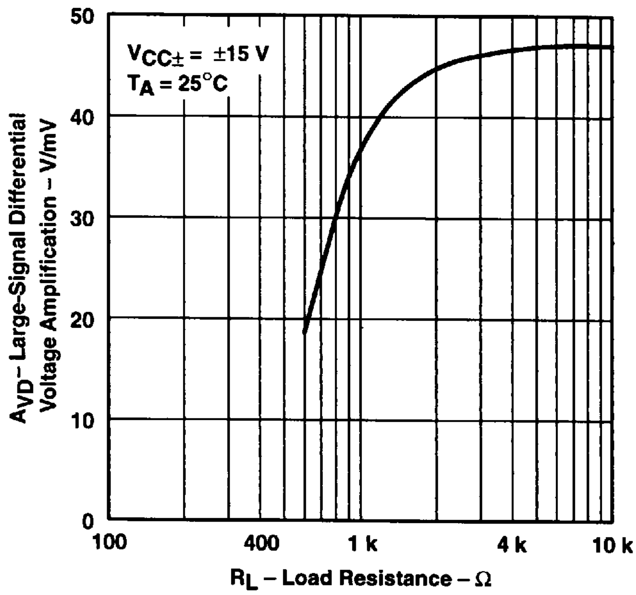


Figure 19

LARGE-SIGNAL DIFFERENTIAL VOLTAGE AMPLIFICATION AND PHASE SHIFT vs FREQUENCY

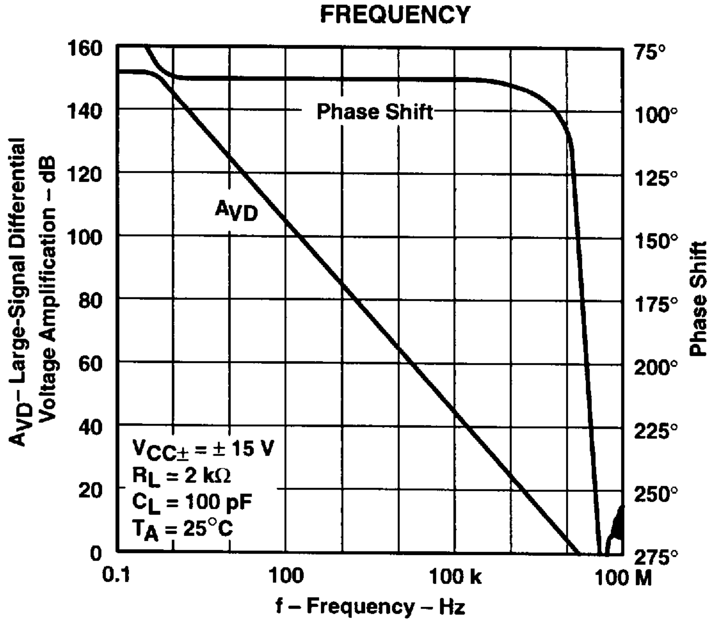


Figure 20

## TYPICAL CHARACTERISTICS

### LARGE-SIGNAL DIFFERENTIAL VOLTAGE AMPLIFICATION AND PHASE SHIFT vs FREQUENCY

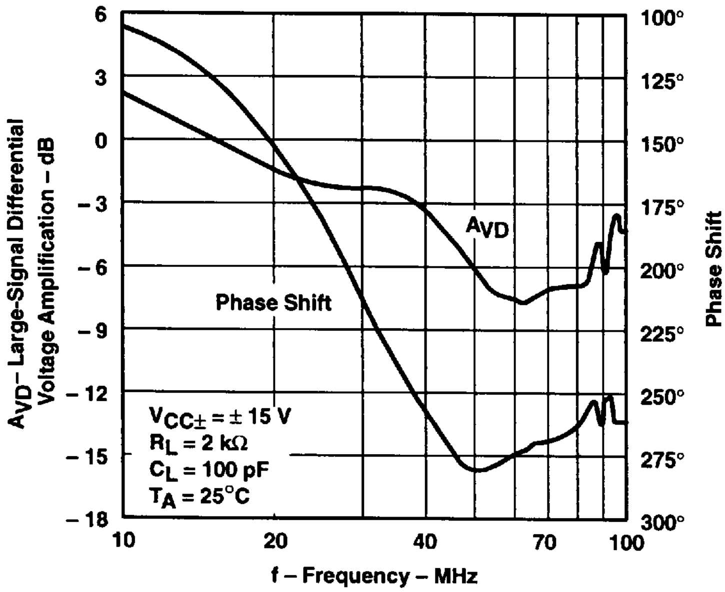


Figure 21

## TYPICAL CHARACTERISTICS

**LARGE-SIGNAL DIFFERENTIAL VOLTAGE AMPLIFICATION† vs FREE-AIR TEMPERATURE**

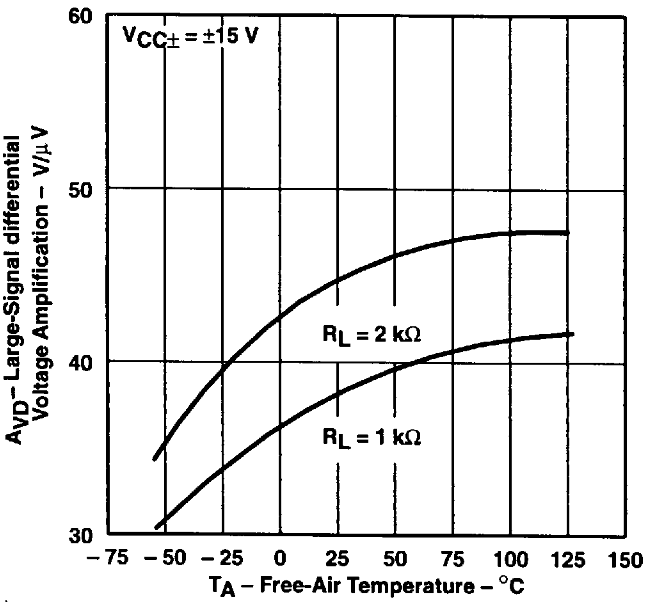


† Data at high and low temperatures are applicable only within the rated operating free-air temperature ranges of the various devices.

**Figure 22**

**OUTPUT IMPEDANCE vs FREQUENCY**

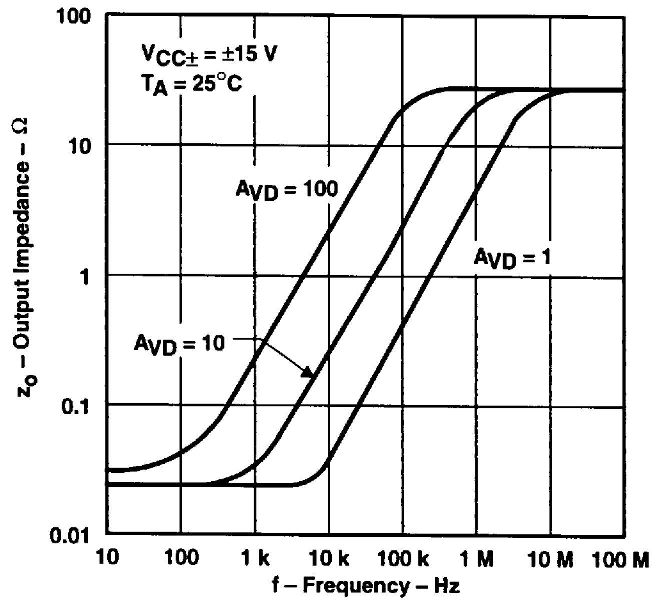


**Figure 23**


TEXAS INSTRUMENTS
POST OFFICE BOX 655303 • DALLAS, TEXAS 75265

## TYPICAL CHARACTERISTICS

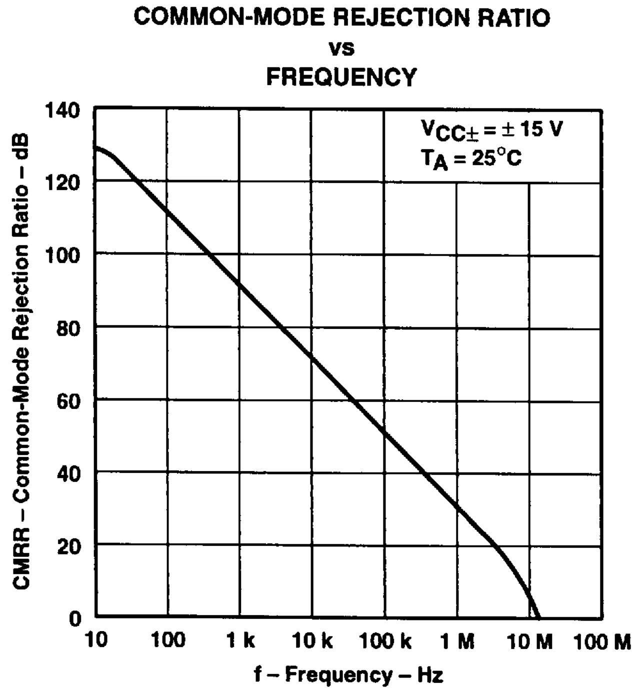


Figure 24

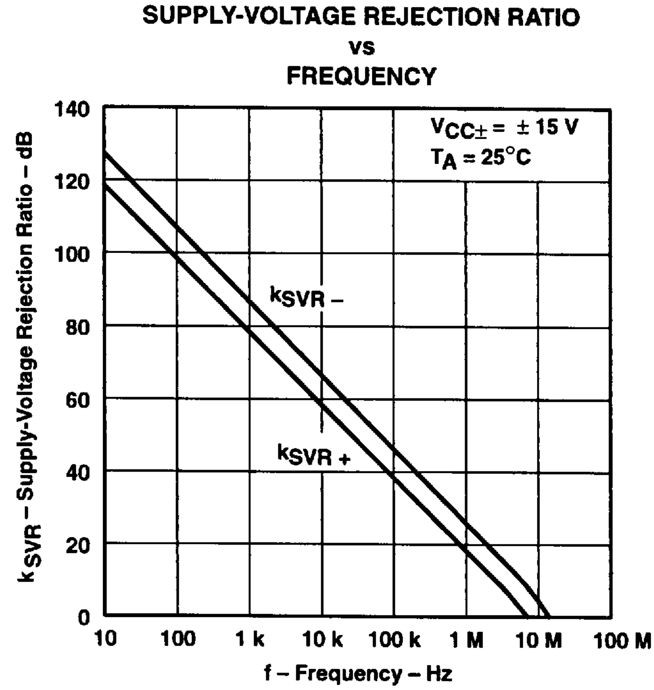


Figure 25

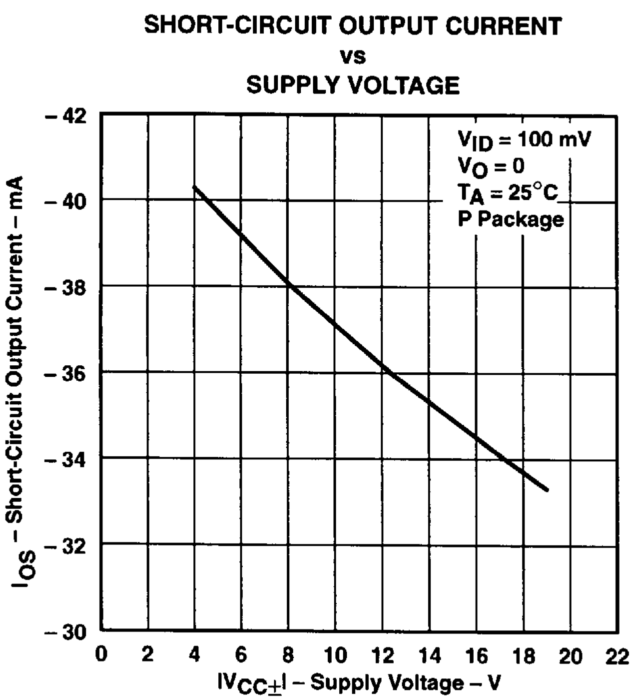


Figure 26

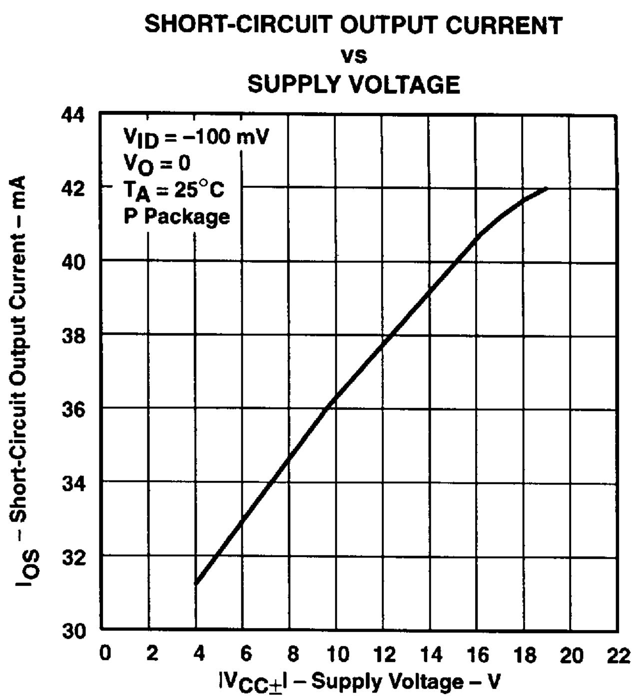


Figure 27

## TYPICAL CHARACTERISTICS

**SHORT-CIRCUIT OUTPUT CURRENT vs ELAPSED TIME**

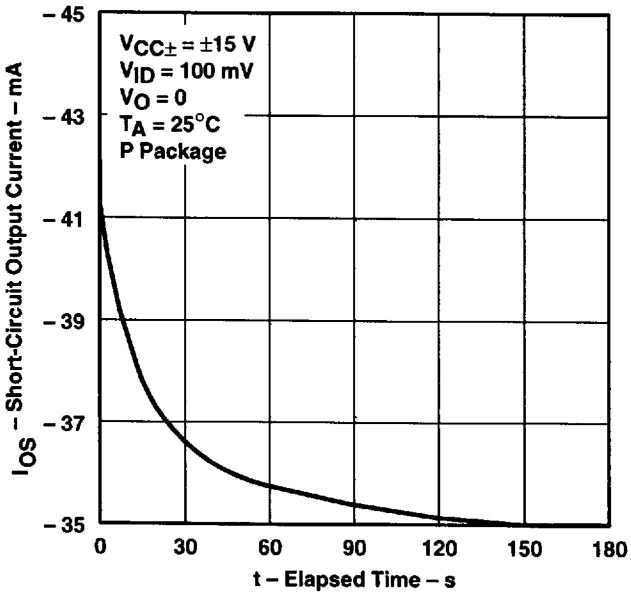


Figure 28

**SHORT-CIRCUIT OUTPUT CURRENT vs ELAPSED TIME**

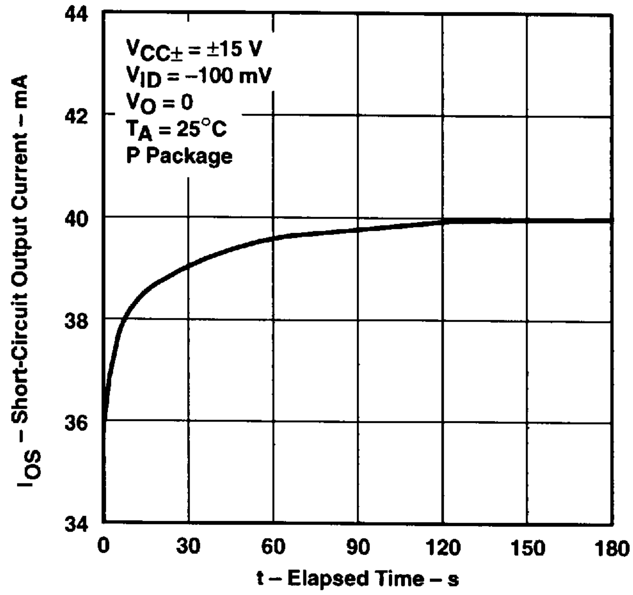


Figure 29

**SHORT-CIRCUIT OUTPUT CURRENT† vs FREE-AIR TEMPERATURE**

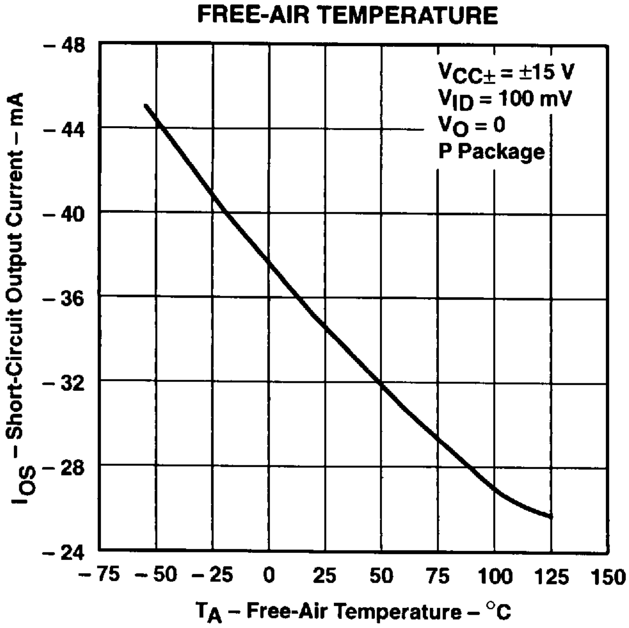


† Data at high and low temperatures are applicable only within the rated operating free-air temperature ranges of the various devices.

Figure 30

**SHORT-CIRCUIT OUTPUT CURRENT† vs FREE-AIR TEMPERATURE**

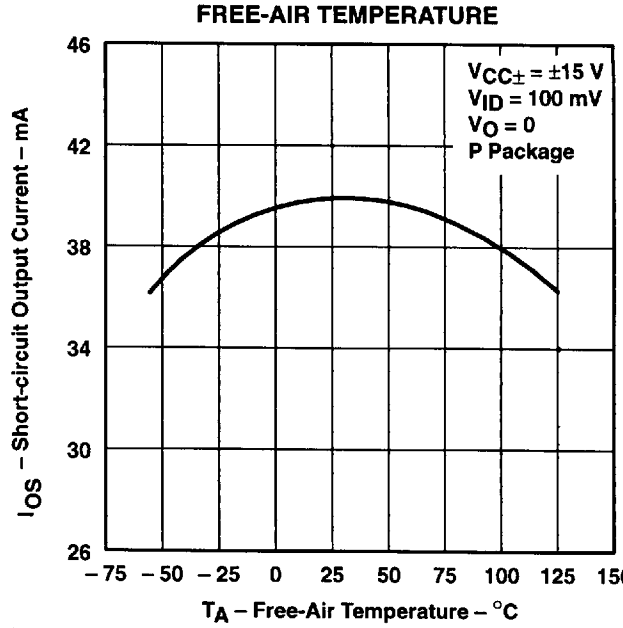


† Data at high and low temperatures are applicable only within the rated operating free-air temperature ranges of the various devices.

Figure 31

## TYPICAL CHARACTERISTICS

SUPPLY CURRENT†
vs
SUPPLY VOLTAGE

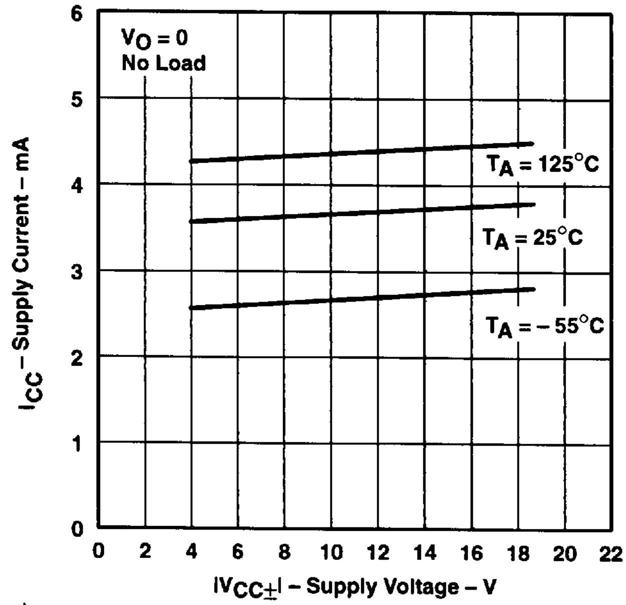


† Data at high and low temperatures are applicable only within the rated operating free-air temperature ranges of the various devices.

Figure 32

SUPPLY CURRENT†
vs
FREE-AIR TEMPERATURE

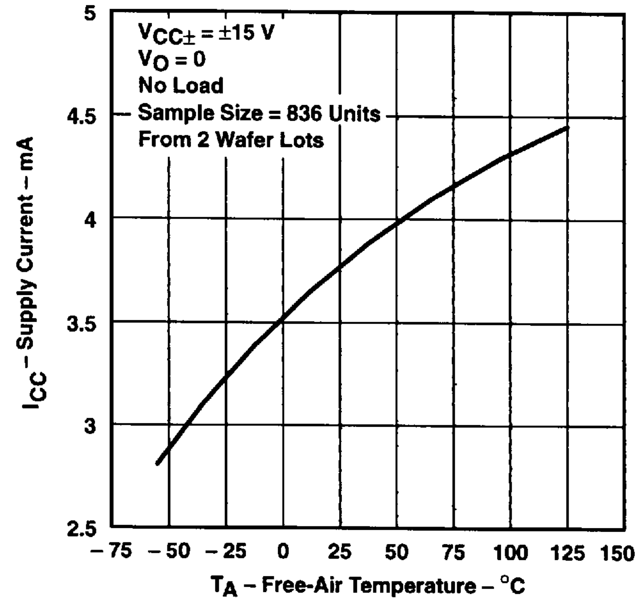


† Data at high and low temperatures are applicable only within the rated operating free-air temperature ranges of the various devices.

Figure 33

VOLTAGE-FOLLOWER
SMALL-SIGNAL
PULSE RESPONSE

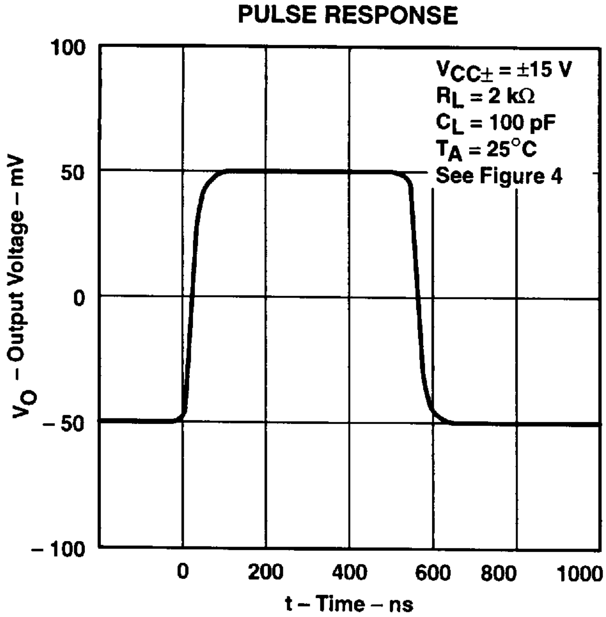


Figure 34

VOLTAGE-FOLLOWER
LARGE-SIGNAL
PULSE RESPONSE

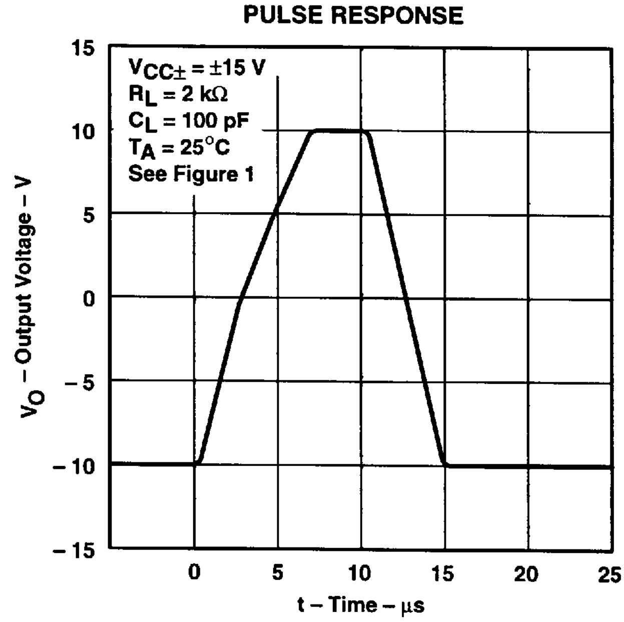


Figure 35

## TYPICAL CHARACTERISTICS

**EQUIVALENT INPUT NOISE VOLTAGE**
**vs**
**FREQUENCY**

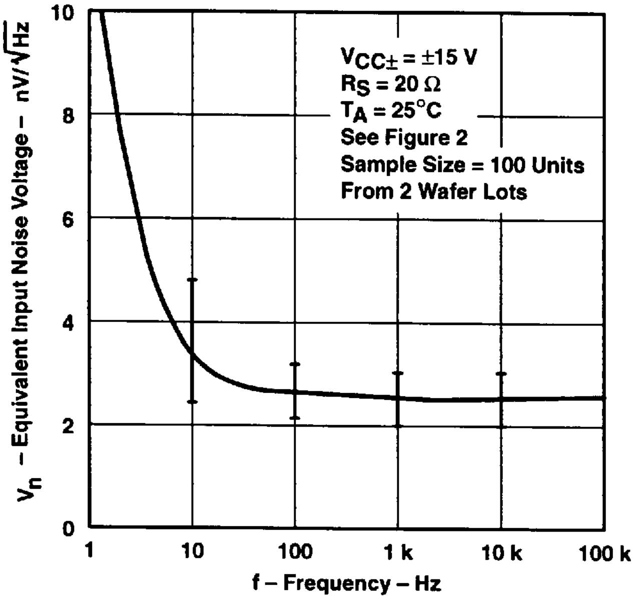


**Figure 36**

**NOISE VOLTAGE**
**(REFERRED TO INPUT)**
**OVER A 10-SECOND INTERVAL**

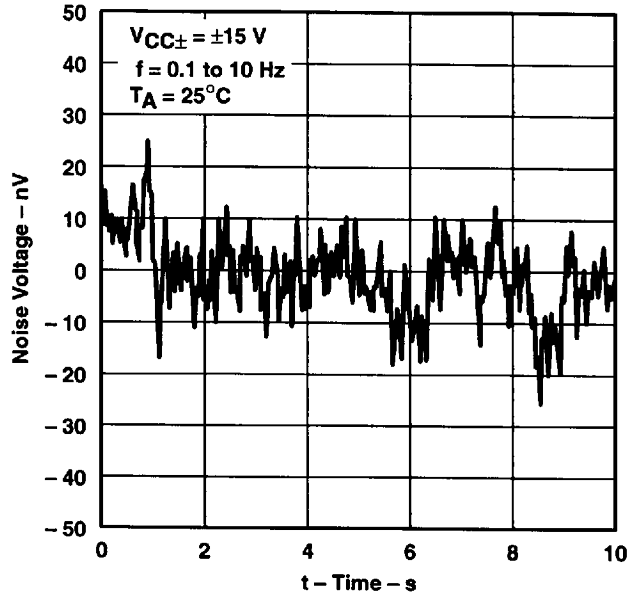


**Figure 37**

**UNITY-GAIN BANDWIDTH**
**vs**
**SUPPLY VOLTAGE**

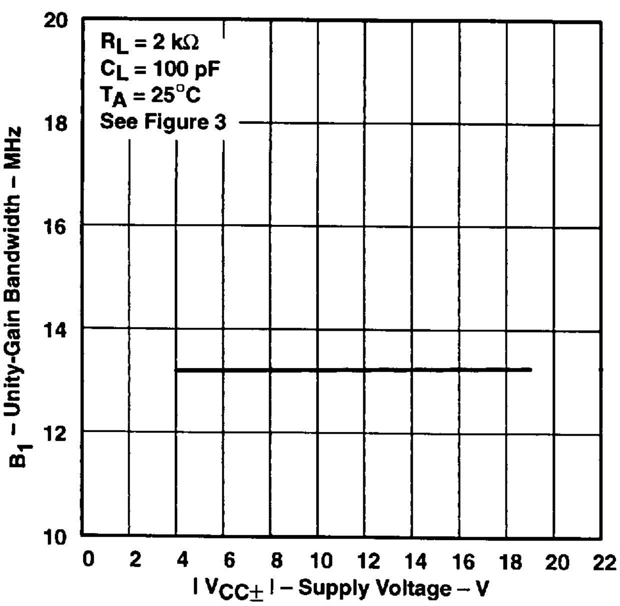


**Figure 38**

**UNITY-GAIN BANDWIDTH**
**vs**
**LOAD CAPACITANCE**

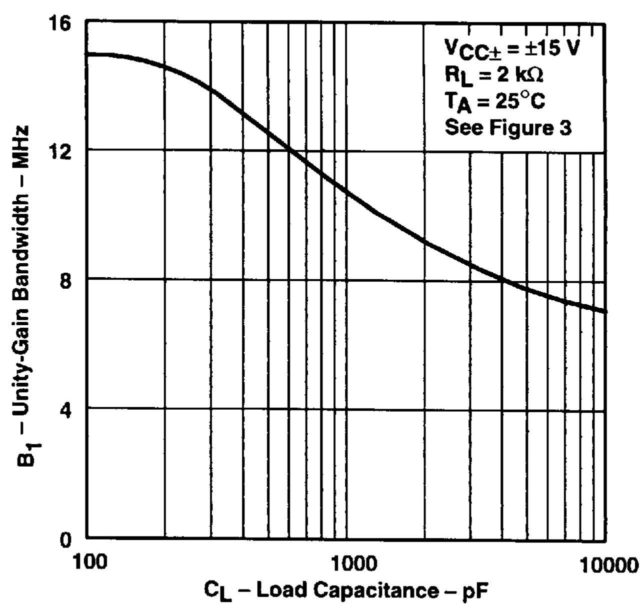


**Figure 39**

## TYPICAL CHARACTERISTICS

**SLEW RATE†**
**vs**
**FREE-AIR TEMPERATURE**

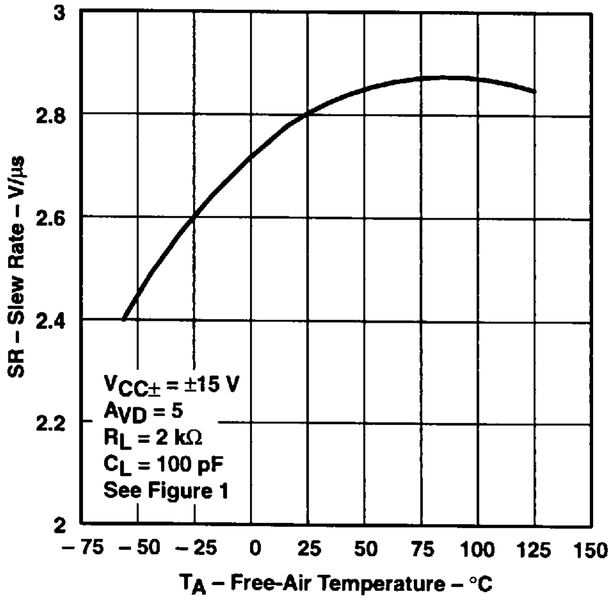


† Data at high and low temperatures are applicable only within the rated operating free-air temperature ranges of the various devices.

**Figure 40**

**PHASE MARGIN**
**vs**
**SUPPLY VOLTAGE**

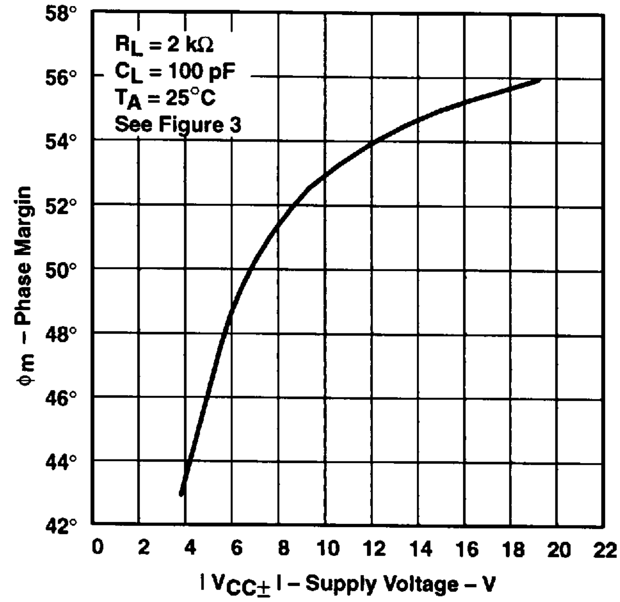


**Figure 41**



8961724 0103625 142

## TYPICAL CHARACTERISTICS

**PHASE MARGIN**
**vs**
**LOAD CAPACITANCE**

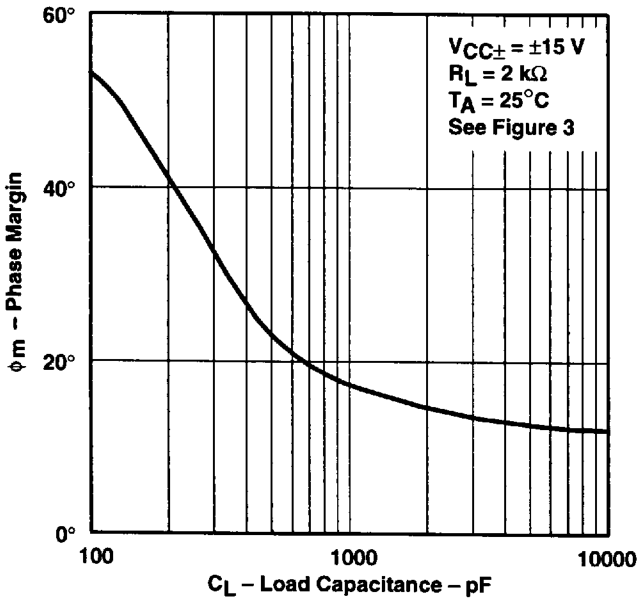


**Figure 42**

**PHASE MARGIN†**
**vs**
**FREE-AIR TEMPERATURE**

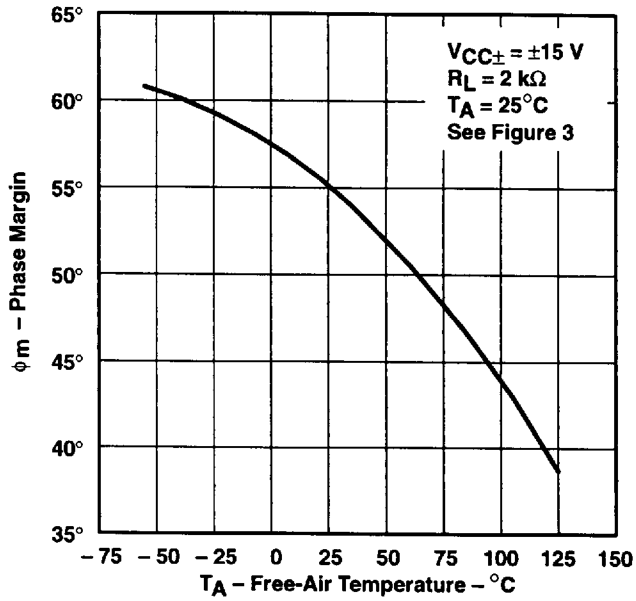


† Data at high and low temperatures are applicable only within the rated operating free-air temperature ranges of the various devices.

**Figure 43**

## APPLICATION INFORMATION

### macromodel information

Macromodel information provided was derived using *PSpice*™ *Parts*™ model generation software. The Boyle macromodel (see Note 6) and subcircuit in Figures 44 and 45 were generated using the TLE2027 typical electrical and operating characteristics at 25°C. Using this information, output simulations of the following key parameters can be generated to a tolerance of 20% (in most cases):

- Maximum positive output voltage swing
- Maximum negative output voltage swing
- Slew rate
- Quiescent power dissipation
- Input bias current
- Open-loop voltage amplification
- Gain-bandwidth product
- Common-mode rejection ratio
- Phase margin
- dc output resistance
- ac output resistance
- Short-circuit output current limit

NOTE 6: G. R. Boyle, B. M. Cohn, D. O. Pederson, and J. E. Solomon, "Macromodeling of Integrated Circuit Operational Amplifiers", *IEEE Journal of Solid-State Circuits*, SC-9, 353 (1974).

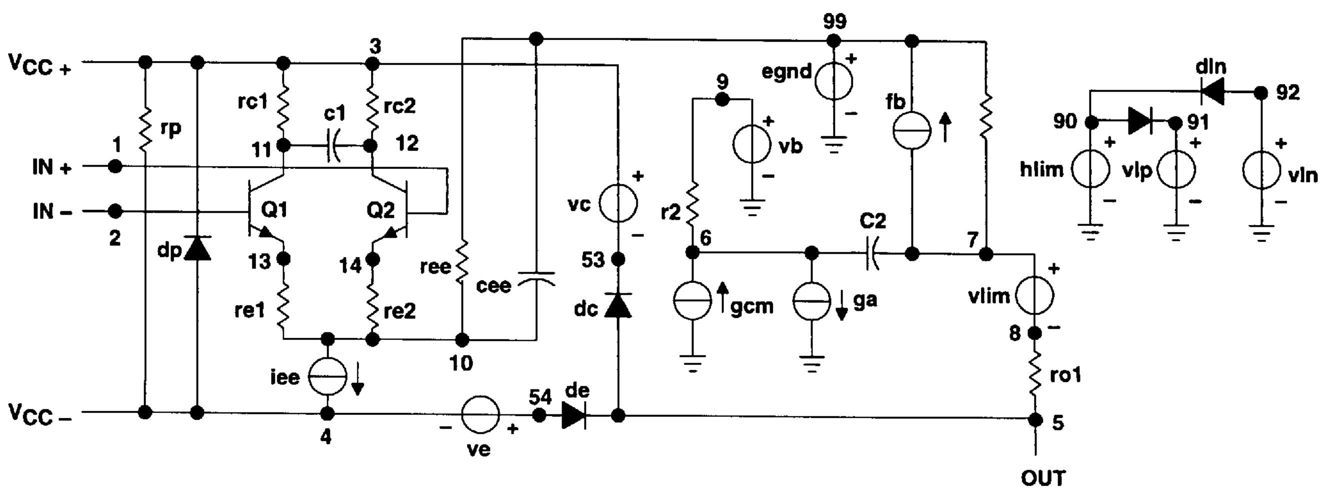


**Figure 44. Boyle Macromodel**

*PSpice* and *Parts* are trademarks of MicroSim Corporation.

## APPLICATION INFORMATION

### macromodel information (continued)

```
.subckt TLE2027 1 2 3 4 5
*
  c1      11  12   4.003E-12
  c2       6   7   20.00E-12
  dc       5  53   dz
  de      54   5   dz
  dlp     90  91   dz
  dln     92  90   dx
  dp       4   3   dz
  egnd    99   0   poly(2) (3,0) (4,0) 0 5 .5
  fb       7  99   poly(5) vb vc ve vlp vln 0 954.8E6 -1E9 1E9 1E9 -1E9
  ga       6   0   11  12   2.062E-3
  gcm      0   6   10  99   531.3E-12
  iee     10   4   dc  56.01E-6
  hlim    90   0   vlim 1K
  q1      11   2   13 qx
  q2      12   1   14 qx
  r2       6   9   100.0E3
  rc1      3  11   530.5
  rc2      3  12   530.5
  re1     13  10   -393.2
  re2     14  10   -393.2
  ree     10  99   3.571E6
  ro1      8   5   25
  ro2      7  99   25
  rp       3   4   8.013E3
  vb       9   0   dc  0
  vc       3  53   dc  2.400
  ve      54   4   dc  2.100
  vlim     7   8   dc  0
  vlp     91   0   dc  40
  vln      0  92   dc  40
.modeldx D(Is=800.0E-18)
.modelqx NPN(Is=800.0E-18 Bf=7.000E3)
.ends
```

**Figure 45. Macromodel Subcircuit**

## APPLICATION INFORMATION

### voltage-follower applications

The TLE2027 circuitry includes input-protection diodes to limit the voltage across the input transistors; however, no provision is made in the circuit to limit the current if these diodes are forward biased. This condition can occur when the device is operated in the voltage-follower configuration and driven with a fast, large-signal pulse. It is recommended that a feedback resistor be used to limit the current to a maximum of 1 mA to prevent degradation of the device. Also, this feedback resistor forms a pole with the input capacitance of the device. For feedback resistor values greater than 10 kΩ, this pole degrades the amplifier phase margin. This problem can be alleviated by adding a capacitor (20 pF to 50 pF) in parallel with the feedback resistor (see Figure 46).

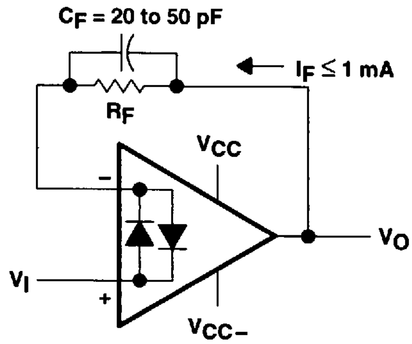


**Figure 46. Voltage Follower**

### Input offset voltage nulling

The TLE2027 series offers external null terminals that can further reduce the input offset voltage. The circuits of Figure 47 can be connected as shown if the feature is desired. If external nulling is not needed, the null terminals may be left disconnected.


(a) STANDARD ADJUSTMENT

(b) ADJUSTMENT WITH IMPROVED SENSITIVITY

**Figure 47. Input Offset-Voltage Nulling Circuits**

## MECHANICAL INFORMATION

**D (R-PDSO-G**)** **PLASTIC SMALL-OUTLINE PACKAGE**

**14 PIN SHOWN**

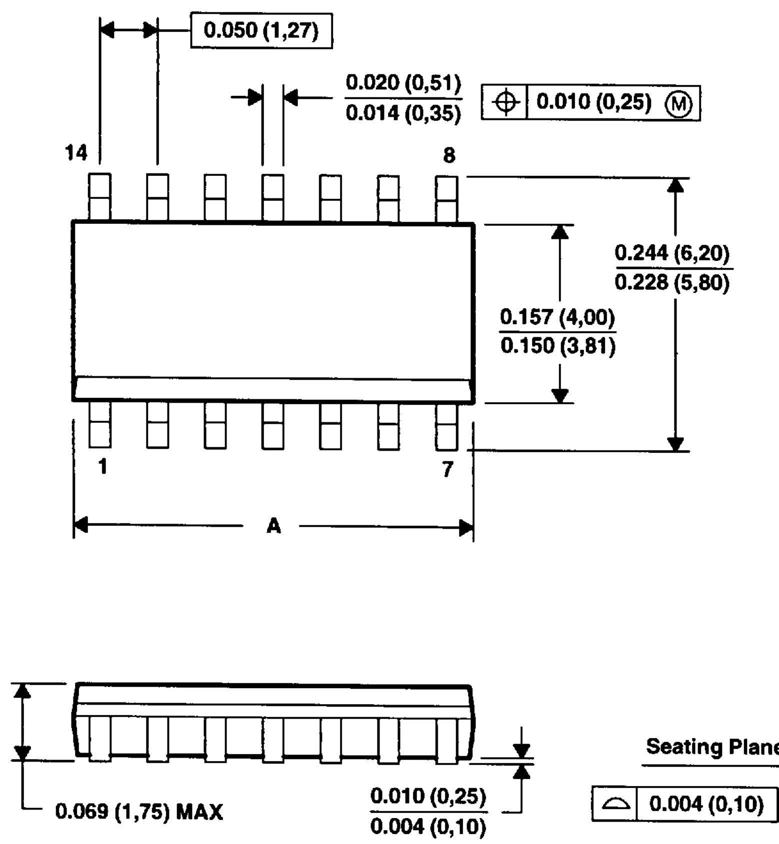


| PINS ** / DIM | 8 | 14 | 16 |
|---|---|---|---|
| A MAX | 0.197 (5,00) | 0.344 (8,75) | 0.394 (10,00) |
| A MIN | 0.189 (4,80) | 0.337 (8,55) | 0.386 (9,80) |

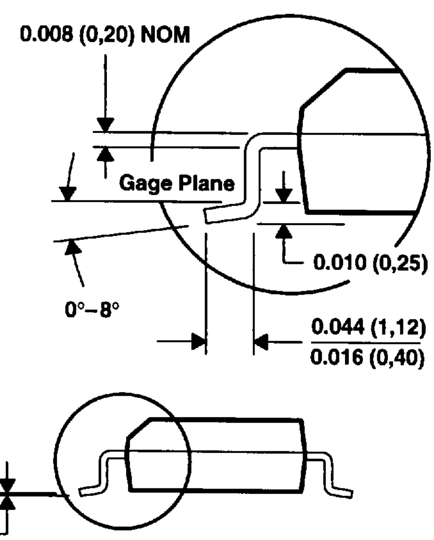


4040047/B 03/95

NOTES: A. All linear dimensions are in inches (millimeters).
B. This drawing is subject to change without notice.
C. Body dimensions do not include mold flash or protrusion, not to exceed 0.006 (0,15).
D. Four center pins are connected to die mount pad.
E. Falls within JEDEC MS-012

## MECHANICAL INFORMATION

**FK (S-CQCC-N**)** **LEADLESS CERAMIC CHIP CARRIER**

**28 TERMINAL SHOWN**

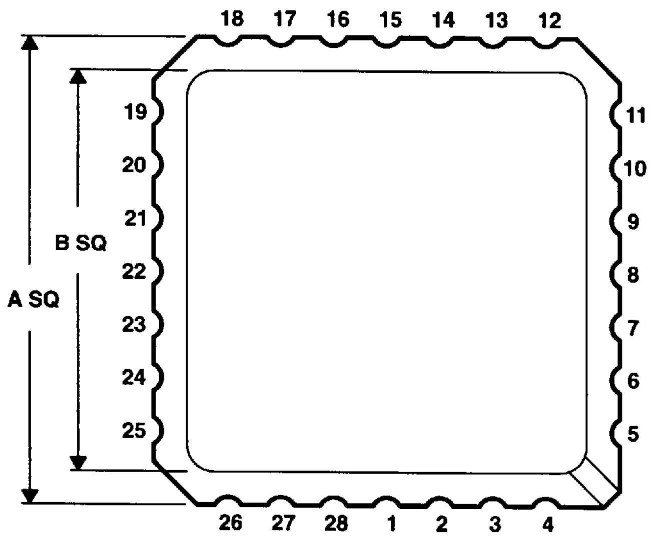


| NO. OF TERMINALS ** | A | | B | |
|---|---|---|---|---|
| | MIN | MAX | MIN | MAX |
| 20 | 0.342 (8,69) | 0.358 (9,09) | 0.307 (7,80) | 0.358 (9,09) |
| 28 | 0.442 (11,23) | 0.458 (11,63) | 0.406 (10,31) | 0.458 (11,63) |
| 44 | 0.640 (16,26) | 0.660 (16,76) | 0.495 (12,58) | 0.560 (14,22) |
| 52 | 0.740 (18,78) | 0.761 (19,32) | 0.495 (12,58) | 0.560 (14,22) |
| 68 | 0.938 (23,83) | 0.962 (24,43) | 0.850 (21,6) | 0.858 (21,8) |
| 84 | 1.141 (28,99) | 1.165 (29,59) | 1.047 (26,6) | 1.063 (27,0) |

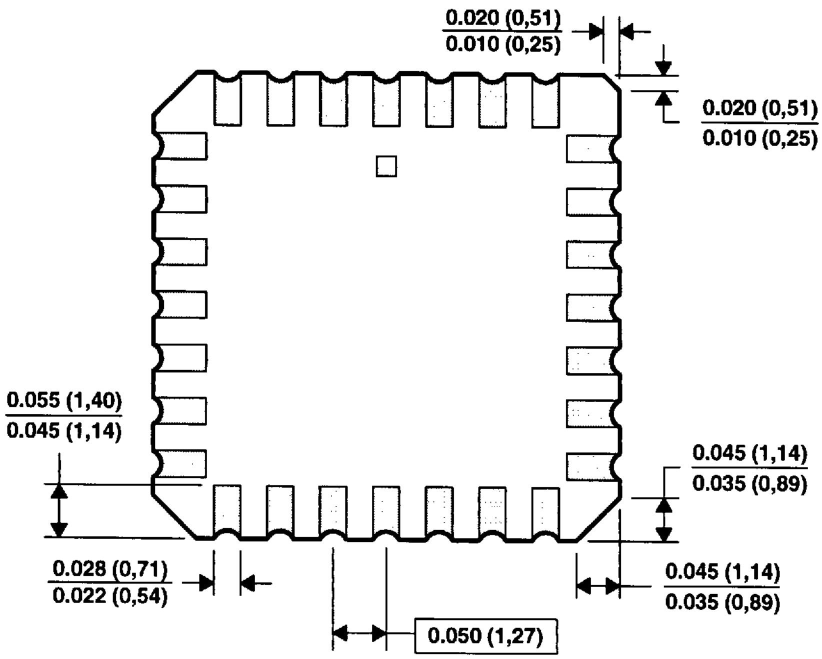


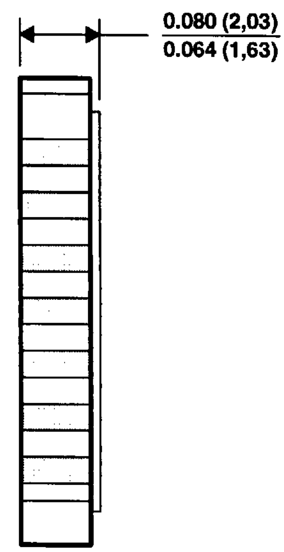


4040140/C 11/95

NOTES: A. All linear dimensions are in inches (millimeters).
B. This drawing is subject to change without notice.
C. This package can be hermetically sealed with a metal lid.
D. The terminals are gold plated.
E. Falls within JEDEC MS-004

## MECHANICAL INFORMATION

**JG (R-GDIP-T8)** **CERAMIC DUAL-IN-LINE PACKAGE**

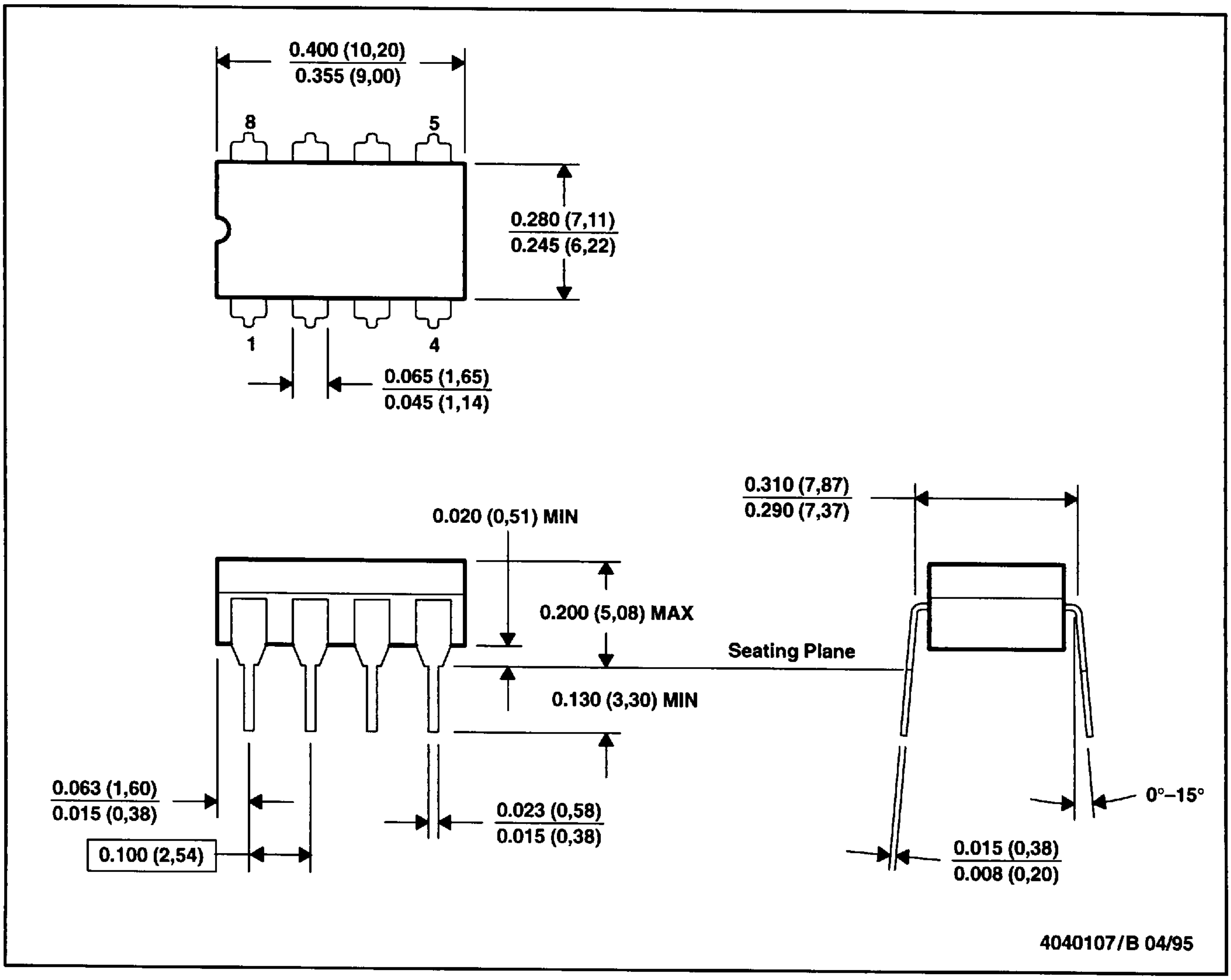


NOTES: A. All linear dimensions are in inches (millimeters).
B. This drawing is subject to change without notice.
C. This package can be hermetically sealed with a ceramic lid using glass frit.
D. Index point is provided on cap for terminal identification only on press ceramic glass frit seal only
E. Falls within MIL-STD-1835 GDIP1-T8

## MECHANICAL INFORMATION

**P (R-PDIP-T8)** **PLASTIC DUAL-IN-LINE PACKAGE**

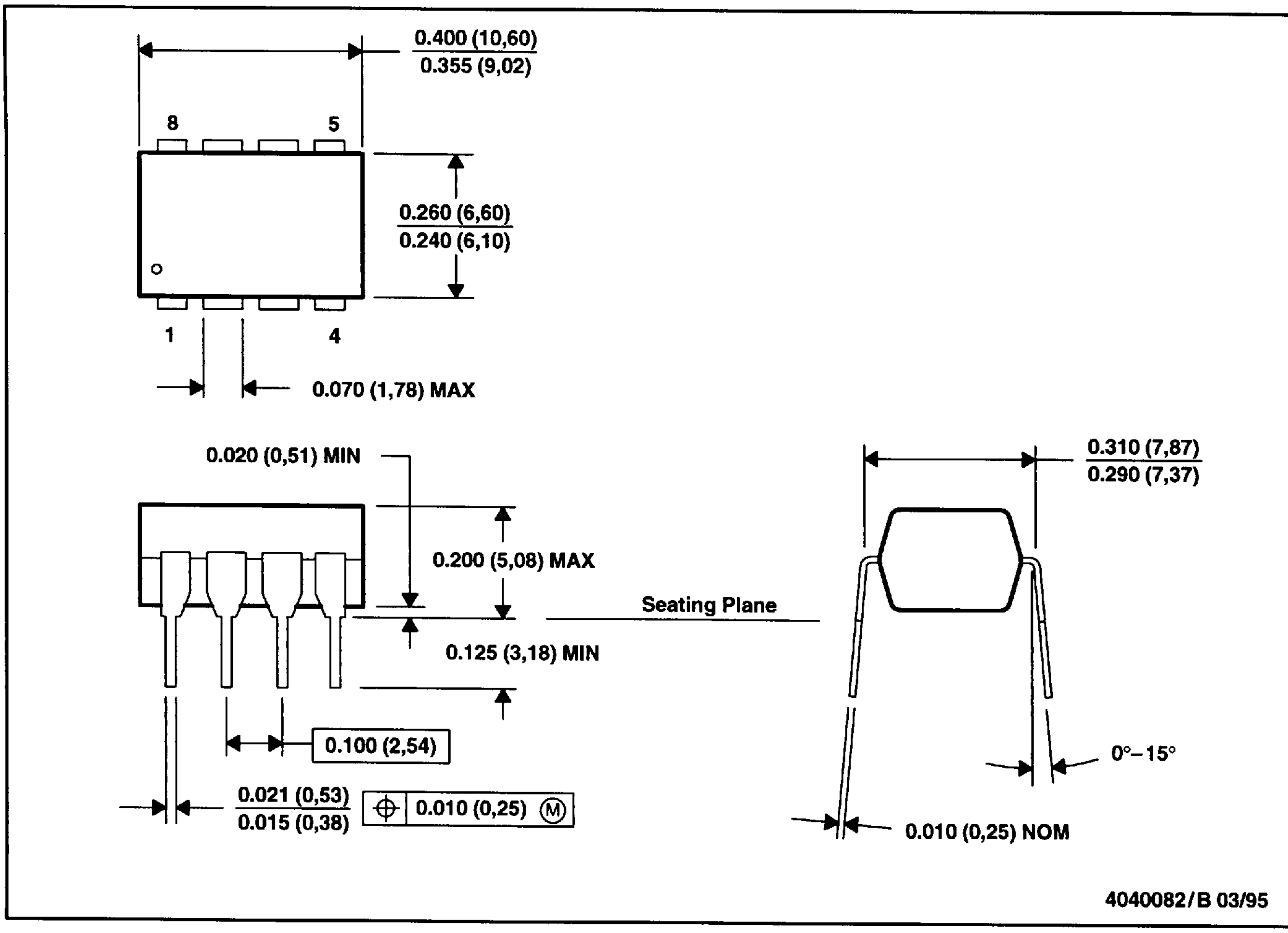


NOTES: A. All linear dimensions are in inches (millimeters).
B. This drawing is subject to change without notice.
C. Falls within JEDEC MS-001